

*E. Wolf, Progress in Optics 44
© 2002 Elsevier Science B.V.
All rights reserved*

Chapter 5

Modulational instability of electromagnetic waves in inhomogeneous and in discrete media

by

Fatkhulla Kh. Abdullaev

*Physical-Technical Institute, Uzbek Academy of Sciences,
G. Mavlyanov str., 2-b, 700084, Tashkent-84, Uzbekistan*

Sergey A. Darmanyán

Institute of Spectroscopy, Russian Academy of Sciences, 142190, Troitsk, Moscow Region, Russia

and

Josselin Garnier

*Laboratoire de Statistique et Probabilité, Université Paul Sabatier,
118 Route de Narbonne, Toulouse Cedex, France*

Contents

	Page
§ 1. Introduction	305
§ 2. MI in homogeneous media	308
§ 3. MI in periodically inhomogeneous media	314
§ 4. MI in random media	332
§ 5. MI in nonlinear discrete optical systems	348
§ 6. Conclusions	361
Acknowledgements	362
References	362

§ 1. Introduction

Modulational instability (MI) represents a fundamental subject in the theory of nonlinear waves. This phenomenon was predicted by Benjamin and Feir [1967] for waves on deep water and by Bespalov and Talanov [1966] for electromagnetic waves in nonlinear media with cubic nonlinearity. The modulational instability phenomenon consists in the instability of nonlinear plane waves against weak long-scale modulations with wavenumbers (frequencies) lower than some critical value. Long time evolution leads to the growth of sidebands and a periodic exchange of energy between a pump and sidebands during the wave propagation. At present, MI is observed in nonlinear optics, plasma physics, condensed matter physics (fibers, magnetics, Bose–Einstein condensates, long Josephson junctions, etc.). This phenomenon is of great interest both for the general theory of nonlinear waves and for applications.

MI exists due to the interplay between the nonlinearity and dispersion/diffraction effects. Important models for investigating MI of electromagnetic waves in nonlinear media represent the scalar and vectorial nonlinear Schrödinger (NLS) equations, the system describing evolution of the envelopes of fundamental and second harmonics waves in quadratically nonlinear media, sine-Gordon equation and others.

In nonlinear optics the MI is of fundamental importance for a formation of both temporal and spatial solitons. MI of the nonlinear continuous-wave (cw) solution of the scalar and vector nonlinear Schrödinger equations has attracted a considerable deal of interest in past years (for overviews see, e.g., books by Agrawal [1995] and Abdullaev, Darmanyan and Khabibullaev [1993]). It has been demonstrated that MI is among the major factors limiting the transmission capacity of long-haul optical communication systems. On the other hand, MI can be used to generate chains of short optical pulses for high-bit-rate data transmission (Hasegawa [1984], Millot, Seve, Wabnitz and Haelterman [1995]).

Much attention has been devoted to investigations of MI in the framework of the NLS equation. The initial stage of the instability can be explored by linear stability analysis, which shows the exponential growth of sidebands. The long-time behavior was investigated by numerical simulations; this approach involves

truncation of a finite number of modes and finding exact periodic solutions of the NLS equation.

Analysis of the long time evolution show that the initial exponential growth of the amplitude of modulations is followed by a decrease, and this process is periodic in time. This phenomenon is analogous to the well-known Fermi–Pasta–Ulam (FPU) recurrence, observed in a chain of coupled nonlinear oscillators. The exact solution of the MI problem expressed via elementary functions has been given by Akhmediev and Korneeov [1986] and Its, Rybin and Sall [1988]; an exact solution in terms of elliptic functions using finite zone potentials theory is by Tracy and Chen [1984]. Recently the FPU recurrence has been observed experimentally in optical fibers by Van Simaey, Emplit and Haelterman [2001].

According to the spatio-temporal analogy, these results can be also applied to beam propagation in bulk nonlinear media and waveguides.

However, all of the above investigations were concerned with MI in homogeneous media. Real systems have different kinds of inhomogeneities, which can strongly affect the process of MI, introducing new phenomena. For example, in optical fibers, in addition to a constant dispersion and nonlinearity, there are effects such as a periodic amplification of pulse and dispersion profiling (or a dispersion compensation) as well as stochastic fluctuations of the dispersion and nonlinearity (for reviews see, e.g., Hasegawa and Kodama [1995], Wabnitz, Kodama and Aceves [1995] and Abdullaev [1999]). In nonlinear photonic crystals the periodic inhomogeneity of linear and nonlinear medium parameters is an intrinsic property. Finally, nonlinear discrete optical systems are also examples of inhomogeneous media. All of these observations motivate the investigation of MI processes in inhomogeneous nonlinear media.

In nonlinear fiber optics the influence of the periodic and random amplification on MI has been studied by Matera, Mecozzi, Romagnoli and Settembre [1993] and Abdullaev [1994]. It was shown that new domains of MI appear in this case; parametric resonance of the unstable mode with the modulation period turned out to be the underlying mechanism. Optical fibers with variable dispersion represent another example of fiber inhomogeneities. Existing long-haul transmission systems frequently consist of different fiber pieces, where the dispersion varies randomly around an averaged value from piece to piece. It has been suggested to use fibers with a controlled dispersion profile (called dispersion-managed fibers) to improve the transmission characteristics of solitons (Smith, Knox, Doran, Blow and Bennion [1996], Gabitov and Turitsyn [1997]). Besides the reduction of soliton jitter and deteriorating effects which can be caused by a periodic amplification, dispersion management may also lead to a decrease of the MI domain as well as MI gain in this domain.

Analogous phenomena occur in fibers with periodic birefringence. This case is described by a vector NLSE with periodic coefficients. The process of MI in random media represents a separate interest. This problem has been considered recently by Karlsson [1998], Abdullaev [1994], Abdullaev, Darmanyan, Kobayakov and Lederer [1996], Abdullaev, Darmanyan, Bischoff and Sørensen [1997] and Abdullaev and Garnier [1999] for fibers with random amplification, dispersion and birefringence.

It should be noted that the problems mentioned above involve inhomogeneities along the evolutionary variable – i.e. the coordinate. Another type of problem occurs in nonlinear optical media with periodic modulations of parameters along a spatial variable which is not evolutionary. A typical example is the dynamics of an electromagnetic wave in a nonlinear optical medium that exhibits periodic variation of linear parameters at a scale comparable to the wavelength of the propagating wave. In this case the inhomogeneities induce the appearance of a reflected wave and we have the dynamics of two interacting waves moving in opposite directions, which is described by the so-called coupled-mode theory. For the investigation of MI it is often useful to apply coupled-mode theory in combination with linear stability analysis (see recent works by De Sterke [1998] and Litchinister, McKinstrie, De Sterke and Agrawal [2001]).

This set of problems also includes the phenomena in nonlinear discrete optical systems, such as arrays of planar waveguides and fibers (see, e.g., the review by Lederer, Darmanyan and Kobayakov [2001]). In such systems, the spreading of the initial excitation due to linear coupling, which can be viewed as effective discrete diffraction, can be compensated by a nonlinearity-induced localization. The array of planar waveguides is described by the discrete NLS equation or by a set of discrete $\chi^{(2)}$ equations, while the array of fibers allowing for the temporal dispersion is represented by a 2D-continuous-discrete NLS equation. Modulation instability in these systems has many new features not observed in homogeneous and continuous media, in particular the critical dependence of both the MI gain and the MI domain on the wavenumber related to the discrete variable. Particular interest which motivates the MI research in these systems is connected with the possibility of generating discrete optical solitons using MI. A similar class of phenomena has been predicted to appear in arrays of Bose–Einstein condensates (BEC) by Abdullaev, Baizakov, Darmanyan, Konotop and Salerno [2001], and in BEC in an optical lattice by Konotop and Salerno [2002].

The structure of this review is as follows. In § 2 we give a description of modulational instability in homogeneous nonlinear media which can be used as a basis for reading of the subsequent sections. This description involves mainly the linear stability analysis which is valid for studying the initial stage of the

evolution of modulations. Methods which admit the description of the long time evolution, such as periodic solutions of the NLS equation and the coupled-mode theory with three modes, are discussed in brief. In § 3 we discuss MI of electromagnetic waves in optical media with periodic inhomogeneities. We start in § 3.1 with MI in optical fibers with periodic amplification, i.e. where the power in the fiber is periodically varied. The structures of sidebands are found and the relation with the sidebands generated by a soliton in such a system is discussed. The analogous problem for a fiber with periodically varying dispersion is considered in § 3.2, and application to dispersion-management optical communication systems is discussed. An important case of MI in periodic nonlinear media, occurring in a Bragg-grating optical fiber, is considered in § 3.3. Coupled-mode theory is employed in order to describe MI in this case. In § 3.4 we consider MI in nonlinear media with periodic potential, while MI in birefringent fibers with periodic dispersion and birefringence is investigated in §§ 3.5 and 3.6. MI in periodic quadratic media is the subject of § 3.7.

In the second part of the review we explore the modulational instability of electromagnetic waves in nonlinear media with random parameters. In § 4.1 we discuss the origin of the random fluctuations of parameters in optical fibers and other nonlinear optical media. MI in fibers with random amplification and dispersion is investigated in §§ 4.2–4.6. MI in randomly birefringent fibers is discussed in § 4.7.

The final part of the review (§ 5) is devoted to the MI of electromagnetic waves in nonlinear discrete optical systems such as an array of planar waveguides and fibers. Particular cases of MI in discrete media with cubic nonlinearity as well as quadratic nonlinearity are investigated.

§ 2. MI in homogeneous media

The phenomenon of instability of long-wavelength modulations of nonlinear plane waves in homogeneous nonlinear media has been predicted in the 1960s for nonlinear optics by Bespalov and Talanov [1966], for water waves by Benjamin and Feir, and for waves in plasma by Vedenov and Rudakov [1964] and Ostrovski [1966]. Later this phenomenon has been observed, among others, for spin waves in magnetics and for waves in nonlinear lattices.

Two important cases for future consideration are MI in Kerr-like media and MI in media with quadratic nonlinearities [$\chi^{(2)}$ media].

2.1. Media with cubic nonlinearity

Let us consider MI in homogeneous optical media with a cubic nonlinearity. Typical example is a nonlinear optical fiber. The evolution of the wave envelope in the fiber is described by the nonlinear Schrödinger equation,

$$i\psi_z + \frac{1}{2}\beta_2\psi_{tt} + \gamma|\psi|^2\psi = 0, \quad (2.1)$$

where z is the propagation distance, t is the time in the moving reference frame, ψ is the envelope of the electromagnetic wave, β_2 is the second-order dispersion coefficient, and γ is the coefficient of the cubic nonlinearity.

By introducing dimensionless variables, this equation can be written in the form

$$iu_z + \frac{1}{2}du_{tt} + |u|^2u = 0. \quad (2.2)$$

Here $d = \pm 1$ corresponds to the cases of anomalous and normal dispersion respectively. This equation has a nonlinear plane-wave solution ψ_c of the form

$$\psi_c = A \exp(iA^2z), \quad (2.3)$$

where without loss of generality A is taken real. Let us investigate the stability of this solution against initial small modulations. If we are interested in the initial stage of the evolution we can apply linear stability analysis. Then we can look for a solution in the form

$$\psi = [A + \psi_1(z, t)] \exp(iA^2z), \quad |\psi_1| \ll A. \quad (2.4)$$

Substituting this equation into eq. (2.2) and linearizing, we get the equation for ψ_1 :

$$i\psi_{1z} + \frac{1}{2}d\psi_{1tt} + A^2(\psi_1 + \psi_1^*) = 0. \quad (2.5)$$

Looking for a solution in the form $\psi_1 \sim \exp(i\Omega t + Kz)$ we get the relation

$$K(\Omega) = \pm\Omega\sqrt{dA^2 - \frac{1}{4}\Omega^2}. \quad (2.6)$$

Thus modulations with frequencies $0 < \Omega < 2A$ are unstable. This is the modulational instability phenomenon that exists in the anomalous dispersion region $d > 0$, but is absent from the normal dispersion region $d < 0$. The MI gain of MI is $|K(\Omega)|$.

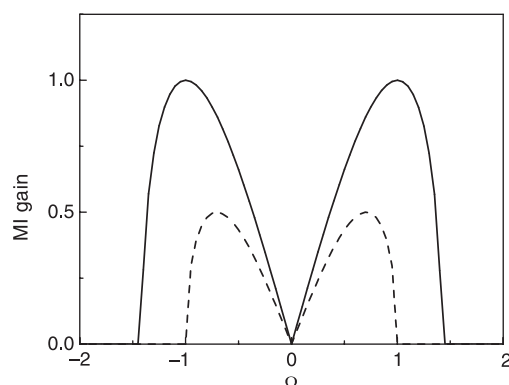


Fig. 1. MI gain versus modulation frequency for the NLS equation in the anomalous dispersion region. The dashed line corresponds to $A = 1$, the solid line to $A = 2$.

In Figure 1 we present the dependence of MI gain on the modulation frequency. In physical units, the maximal gain is at $\Omega_m = \pm\sqrt{2\gamma A^2/|\beta_2|}$ and $K_m = \gamma A^2$. MI in an optical fiber has been observed experimentally by Tai, Hasegawa and Tomita [1986]. The solution (2.6) describes MI in conservative media. For nonconservative media the linearized equation can be solved too. For example, the problem of MI in fibers with two-photon absorption can be solved exactly (see the work by Tsoy, De Sterke and Abdullaev [2001]). More information can be found in books by Abdullaev, Darmanyan and Khabibullaev [1993], Agrawal [1995] and Hasegawa and Kodama [1995].

The long time evolution of the modulated wave requires to find a periodic solution of the NLS equation. In general the solution requires the application of the finite zone potentials theory. Here we analyze, following Akhmediev and Korneev [1986] and Akhmediev, Eleonsky and Kulagin [1990], the simple periodic solution of the NLS equation describing the evolution of a nonlinear plane wave on which a small periodic solution is superimposed.

Introducing the new field as $u \rightarrow ue^{iz}$ and representing the solution as $u = v + iw$ we can rewrite eq. (2.2) as a system of equations for two real functions. Assume that these functions are coupled by the *linear* relation

$$v = \eta(z)(w + 1),$$

where $\eta = -\tanh z$, we obtain the Bernoulli equation for the function w :

$$w_z + \tanh(z)w^2 + \tanh(z)w = 0. \quad (2.7)$$

Thus the solution of eq. (2.2) is

$$u(z, t) = \frac{-\sqrt{2} \sinh(z) + i \cos(\sqrt{2}(t - t_0))}{\sqrt{2} \cosh(z) - \cos(\sqrt{2}(t - t_0))}. \quad (2.8)$$

This time-periodic solution of the NLS equation can also be obtained using the Darboux dressing method for the nonlinear plane-wave solution (2.2) (see the article by Its, Rybin and Sall [1988]).

The solution (2.8) coincides with the solution obtained from the linear stability analysis at $z \rightarrow -\infty$:

$$u \approx 1 + \left[a \left(1 + i \frac{2\delta}{\Omega^2} \right) e^{\delta z} + b \left(1 - i \frac{2\delta}{\Omega^2} \right) e^{-\delta z} \right] \cos(\Omega(t - t_0)), \quad (2.9)$$

with $b = 0$. Here $\delta = \Omega\sqrt{1 - \Omega^2/4}$ is the gain, and a, b are small independent parameters defined by the initial modulation. At $z \rightarrow \infty$ the solutions (2.8) and (2.9) coincide when $a = 0$, $\Omega = \sqrt{2}$, and there is an additional multiplier $e^{i\pi}$. Thus, during the instability the amplitude grows to the maximal value at $z = 0$ and then evolves at $z \rightarrow \infty$ to the nonlinear plane-wave solution with the initial amplitude and opposite phase.

The recurrence phenomenon can be described considering a finite number of modes. As shown by Infeld [1981], Infeld and Rowlands [1990] and Trillo and Wabnitz [1991], a three-mode approximation for the periodic solution of the NLS equation is effective. These modes are the carrier and the first two sidebands at frequencies $\omega \pm \Omega$. Thus in this approximation the field can be written as

$$u(z, t) = u_0(z) + u_{-1}(z) e^{i\Omega t} + u_1(z) e^{-i\Omega t}. \quad (2.10)$$

Here u_0 is the carrier amplitude, and u_{-1}, u_1 are the amplitudes of the sidebands at $\omega - \Omega$ and $\omega + \Omega$.

Using eqs. (2.10) and (2.2) we find the system for the amplitudes of the modes:

$$\begin{aligned} iu_{0z} + (2|u_{-1}|^2 + 2|u_1|^2 + |u_0|^2)u_{-1} + 2u_0^*u_{-1}u_1 &= 0, \\ iu_{-1z} - \frac{1}{2}\Omega^2u_{-1} + (2|u_0|^2 + 2|u_1|^2 + |u_{-1}|^2)u_{-1} + u_0^2u_1^* &= 0, \\ iu_{1z} - \frac{1}{2}\Omega^2u_1 + (2|u_0|^2 + 2|u_{-1}|^2 + |u_1|^2)u_1 + u_0^2u_{-1}^* &= 0. \end{aligned} \quad (2.11)$$

Writing the modes as $u_k = |u_k|e^{i\phi_k}$, introducing variables $\eta = |u_0|^2/(|u_{-1}|^2 + |u_1|^2 + |u_0|^2)$, $\phi = \phi_{-1} + \phi_1 - 2\phi_0$, and using two conserved quantities of eq. (2.11), we obtain the equations for η and ϕ :

$$\eta_z = -2\eta(1 - \eta) \sin(\phi), \quad \phi_z = -2(1 - 2\eta) \cos(\phi) + 3\eta + \kappa - 1. \quad (2.12)$$

The corresponding Hamiltonian is

$$H = 2\eta(1 - \eta) \cos(\phi) - (\kappa - 1) \eta - \frac{3}{2} \eta^2. \quad (2.13)$$

The numerical simulation of the full NLS equation and eqs. (2.12) with the same initial modulation shows good agreement. In particular, the reduced system describes the recurrence phenomena very well (Trillo and Wabnitz [1991]).

2.2. Media with quadratic nonlinearity

The second example of importance for the following subsections is MI in media with a quadratic nonlinearity (Trillo and Ferro [1995]). The governing equations, describing the propagation of the envelopes of the fundamental wave (FW) and the second harmonics (SH) in dimensionless variables are

$$\begin{aligned} iu_z + \frac{1}{2}\beta_1 u_{tt} + u^* v \exp(i\delta kz) &= 0, \\ iv_z + i\nu_g v_t + \frac{1}{2}\beta_2 v_{tt} + \frac{1}{2}u^2 \exp(-i\delta kz) &= 0. \end{aligned} \quad (2.14)$$

Here $z = x/x_d$, $x_d = t_0^2/|\beta_1|$ is the dispersion length, t is the time in the moving reference frame, and δk is the dimensionless wave-vector mismatch.

Looking for solutions of the form

$$u = u_0 \exp(i\phi_1), \quad v = v_0 \exp(i\phi_2), \quad \phi_{1,2} = \mu_{1,2}z,$$

we obtain the stationary solution

$$u_0 = \pm \sqrt{2\mu(2\mu - \delta k)}, \quad v_0 = \mu, \quad (2.15)$$

where $\mu_1 = \mu$. Here we have taken into account that $\mu_2 = 2\mu_1 - \delta k$. The total intensity is normalized to 1, $\frac{1}{2}|u|^2 + |v|^2 = 1$, thus μ^2 represents the fraction of SH mode in the total intensity. The relation for the phases is

$$\phi_1 = \nu_0 z \phi_2 = \frac{u_0^2}{2\nu_0} z.$$

Dispersion and nonlinearity can lead to MI of cw solutions (2.15) against small perturbations. To study MI let us consider the ansatz

$$u = (u_0 + u_1(z, t)) \exp(i\mu z), \quad v = (v_0 + v_1(z, t)) \exp(2\mu - \delta k). \quad (2.16)$$

Inserting these expressions into eqs. (2.14) and retaining only terms of first order in perturbations we get the set

$$\begin{aligned} iu_{1z} + \frac{1}{2}\beta_1 u_{1tt} - \mu u_1 + \nu_0 u_1^* + u_0 v_1 &= 0, \\ iv_{1z} + i\nu_g v_{1t} + \frac{1}{2}\beta_2 v_{1tt} - 2\mu v_1 + u_0 u_1 &= 0. \end{aligned} \quad (2.17)$$

Looking for solutions of this linear system of partial differential equations in the form

$$\begin{aligned} u_1 &= A(z) \exp(i\Omega t) + B(z) \exp(-i\Omega t), \\ v_1 &= C(z) \exp(i\Omega t) + D(z) \exp(-i\Omega t), \end{aligned} \quad (2.18)$$

we arrive at the linear problem

$$\frac{d\mathbf{A}}{dz} = \mathbf{M}\mathbf{A},$$

where $\mathbf{A} = (A, B, C, D)^T$ and the complex matrix \mathbf{M} is

$$\mathbf{M} = i \begin{bmatrix} -\Omega_1^2 & \nu_0 & u_0 & 0 \\ -\nu_0 & \Omega_1^2 & 0 & -u_0 \\ u_0 & 0 & -\Omega_2^2 - \nu_g \Omega & 0 \\ 0 & -u_0 & 0 & \Omega_2^2 - \nu_g \Omega \end{bmatrix} \quad (2.19)$$

with

$$\Omega_1^2 = \frac{1}{2}\beta_1 \Omega^2 + \mu, \quad \Omega_2^2 = \frac{1}{2}\beta_2 \Omega^2 + \mu_2.$$

MI occurs if an eigenvalue with a positive real part exists. For a group-velocity matched process, i.e. for $\nu_g = 0$, the eigenvalues are

$$2K^\pm = \sqrt{f} \pm \sqrt{f^2 - f_1}, \quad (2.20)$$

where

$$\begin{aligned} f &= -2(\mu_2^2 + 4\mu_2\mu) - 2(\beta_2\mu_2 + \beta_1\mu)\Omega^2 - \frac{1}{2}(\beta_1^2 + \beta_2^2)\Omega^4, \\ f_1 &= \Omega^2 [\beta_1^2\beta_2^2\Omega^6 + 4\beta_1\beta_2(\beta_2\mu + \beta_1\mu_2)\Omega^4 + 4\beta_1^2\mu_2^2\Omega^2 - 16\mu(\beta_1\mu_2^2 + 2\beta_2\mu_2\mu)]. \end{aligned}$$

Analysis of this equation shows that MI develops for both normal and anomalous dispersion regions.

In the normal dispersion regime, where $\beta_{1,2} < 0$, MI exists in the region of frequencies

$$\Omega_d^2 < \Omega^2 < \Omega_u^2,$$

$$\Omega_d^2 = \frac{1}{|\beta_2|}[(\mu_2^2 + 8|\beta_2|\mu_2\mu)^{1/2}], \quad \Omega_u^2 = \frac{2}{|\beta_2|}(\mu_2 + 2|\beta_2|\mu).$$

For the case $\delta k = 2$ the peak of the gain is achieved at the frequency $\Omega = \sqrt{2}$. This value can be obtained also from the phase-matching condition $k_p = k_a + k_s$. This is the condition for the decay of an SH photon with wavevector k_p into Stokes (k_s) and anti-Stokes (k_a) photons. With decreasing δk the gain band narrows and the gain decreases.

In the anomalous dispersion region, $\beta_{1,2} > 0$, MI occurs for

$$0 < \Omega^2 < \Omega_d^2. \quad (2.21)$$

For $\delta k = 2$ the eigenmode is stable, and in the case of a pump with $\phi = \pi$ for $\delta k = -2$ it is unstable. More details can be found in the articles by Trillo and Ferro [1995] and He, Drummond and Malomed [1996].

§ 3. MI in periodically inhomogeneous media

3.1. MI in optical fibers with periodic nonlinearity

The governing wave equation for the envelope of the electric field in a Kerr-like nonlinear medium with a periodic nonlinearity has the form

$$iu_z + d_0 u_{tt} + 2f(z)|u|^2 u = 0, \quad (3.1)$$

where $d_0 = \pm 1$ for anomalous and normal group dispersion, respectively, and $f(z)$ describes the periodic modulations of the fiber's nonlinear parameters. These modulations are induced either by periodic variations of the effective core area

A_{eff} of the fiber along z , or by periodically positioned amplifiers. This equation has the steady-state cw solution

$$v = A \exp(i\phi), \quad \phi = 2A^2 \int_0^z f(z') dz'. \quad (3.2)$$

Without loss of generality we can take A real. Let us consider the stability of the wave solution (3.2) with respect to small modulations

$$v = [A + \psi(z, t)] \exp(i\phi), \quad |\psi| \ll A. \quad (3.3)$$

Substituting eq. (3.3) into eq. (3.2) and linearizing with respect to the correction ψ , we obtain the equation for $\psi(x, t)$:

$$i\psi_z + d_0 \psi_{tt} + 2A^2 f(z) (\psi + \psi^*) = 0. \quad (3.4)$$

By expressing ψ as

$$\psi = C(z) \exp(i\Omega t) + B^*(z) \exp(-i\Omega t) \quad (3.5)$$

and inserting eq. (3.5) into eq. (3.4), we obtain the system of equations

$$ib_z - d_0 \Omega^2 c = 0, \quad (3.6)$$

$$ic_z - d_0 \Omega^2 b + 4f(z) A^2 b = 0, \quad (3.7)$$

where $c(z) = C(z) - B(z)$ and $b(z) = C(z) + B(z)$. This system can be reduced to

$$b_{zz} + \Omega^2 [\Omega^2 - 4d_0 A^2 f(z)] b = 0. \quad (3.8)$$

Choosing for the variation the particular form $f(z) = 1 - f_0 \cos(az)$, $f_0 \ll 1$, we obtain the Mathieu equation instead of eq. (3.8) (Abdullaev [1994], Matera, Mecozzi, Romagnoli and Settembre [1993]):

$$b_{zz} + \omega_0^2 [1 + h \cos(az)] b = 0, \quad (3.9)$$

where

$$h = \frac{4A^2 f_0 d_0}{\Omega^2 - 4d_0 A^2}, \quad \omega_0^2 = \Omega^2 (\Omega^2 - 4A^2 d_0). \quad (3.10)$$

By applying the standard method (Landau and Lifshitz [1973]) for the case $0 < h \ll 1$, we find that the wave is unstable in the region of parametric

resonance, which occurs when $\omega_0 = \frac{1}{2}ma$, with $m = 1, 2, 3, \dots$. In the region of the first parametric resonance we have $a = 2\omega_0$; i.e. the wave is unstable for modulations with frequency

$$\Omega^2 = 2A^2d_0 + \sqrt{4A^4 + \frac{1}{4}a^2}. \quad (3.11)$$

The width δ of the MI region can be found from the instability condition for the solution of eq. (3.9):

$$|\delta| < \frac{2f_0A^2\Omega}{\sqrt{\Omega^2 - 4d_0A^2}}. \quad (3.12)$$

The corresponding width $\Delta\Omega$ is found from eqs. (3.11) and (3.12):

$$\Delta\Omega \approx \frac{d_0f_0a^2}{\Omega \left(\sqrt{\Omega_0^4 + a^2} - \Omega_0^2 \right) \sqrt{\Omega_0^4 + a^2}}, \quad (3.13)$$

where $\Omega_0^2 = 4A^2d_0$. The appearance of a new MI region at higher modulation frequencies indicates that it is possible to generate a chain of ultrashort pulses with a high repetition rate. It can be shown that the maximum gain g_{\max} for parametric resonance in the region of anomalous group-velocity dispersion when $a \gg 4A^2$, is equal to

$$g_{\max} \approx f_0A^2. \quad (3.14)$$

For small $a \ll 4A^2$ we have

$$g_{\max} \approx \frac{8f_0A^4}{a}. \quad (3.15)$$

For the normal dispersion domain $a \gg \Delta = 4A^2$ we can use the estimate

$$\Omega \approx \sqrt{\frac{1}{2}a - 2A^2}. \quad (3.16)$$

For small $a \ll \delta$, Ω is approximated by

$$\Omega \approx \frac{a}{8A}. \quad (3.17)$$

Let us now estimate the value of the effect for the case of periodic variation of amplification in fibers (Matera, Mecozzi, Romagnoli and Settembre [1993]). The governing equation is

$$iv_z + dv_{tt} + 2|v|^2v = -i\Gamma v,$$

where Γ is the loss coefficient. In each amplifier point the loss is exactly compensated. Let us perform in the interval $[0, l]$, with l the distance between

amplifiers, the transformation $u = v \exp(-\Gamma z)$. Then we have eq. (3.1) with $f(z) = \exp(-2\Gamma z)$ in the interval $0 < z < l$ and periodic with period l . If we take the first terms of the Fourier expansion for $f(z)$,

$$f(z) = \sum_{n=-\infty}^{\infty} \frac{(1 - e^{-2\Gamma l})}{(2\Gamma l)[1 - in\pi/(\Gamma l)]} \exp\left(-i\frac{2\pi n}{l}z\right),$$

for the case $\Gamma l \ll 1$, we obtain the model for $f(z)$ as

$$f(z) \approx 1 + \frac{2\Gamma l}{\pi} \sin\left(\frac{2\pi z}{l}\right).$$

In the dimensional units of eq. (2.1) with $d_0 = -2 \text{ ps}^2 \text{ km}^{-1}$, $\gamma = 2 \text{ W}^{-1} \text{ km}^{-1}$, $\Gamma = 0.03 \text{ km}^{-1}$, $l = 10 \text{ km}$, $P = 0.1 \text{ W}$ and $f_0 = 0.2$, the critical value of Ω is approximately 0.67 THz , and the increment $g_{\max} \approx 0.1 \text{ km}^{-1}$.

For $\Gamma l \geq 1$ the position of sidebands is

$$\Omega_p = \pm \sqrt{\frac{\pi p}{dl} - \frac{2A^2 c_0}{d}}, \quad p = 0, 1, 2, \dots, \quad (3.18)$$

where $c_0 = [1 - \exp(-2\Gamma l)]/(2\Gamma l)$. The positions of sidebands for $|p| = 1$ and $d = -0.5 \text{ ps}^2 \text{ km}^{-1}$, $P = 1.5 \text{ mW}$, $\gamma = 3 \times 10^{-3} \text{ mW}$, $\Gamma = 0.03 \text{ km}^{-1}$ and $l = 100 \text{ km}$ are 40 GHz from the central frequency. Numerical simulation of the amplitude gain in the amplifier chain after 10000 km gives the value $\sim 10^{-3} \text{ km}^{-1}$. Experimental observation of sideband generation upon periodic variation of power in a fiber has been reported by Kikuchi, Lorattanasane, Futami and Kaneko [1995].

It should be noted that this type of instability is different from the sideband instability occurring for optical soliton propagation in a fiber with periodic variation of power (Matera, Mecozzi, Romagnoli and Settembre [1993], Gordon [1992], Kelley [1992]). When a soliton propagates in such a fiber, the periodic variation of the nonlinear coefficient leads to the generation of radiation corresponding to the sidebands in the spectrum of soliton, with frequencies

$$\Omega_n = -\frac{1}{\tau^2} + \frac{4\pi n}{|\beta_2|l},$$

where τ is the initial duration of the pulse. MI is a parametric resonance and exists both for even and for odd values of n , but the emission generated by the soliton is due to the resonant process between the soliton with wavevector

$|\beta_2|/(2\tau^2)$ and a dispersive wave with wavevector $|\beta_2|\Omega^2/2$ under periodic modulation with wavevector $2\pi/l$, and exists only for even values of n .

3.2. MI in fibers with periodic dispersion

It has been observed that a new type of soliton can exist in fibers with a periodic variation of the dispersion along the fiber. Remarkably, these solitons exist also in the region of normal averaged dispersion. These solitons, called dispersion-managed (DM) solitons, have enhanced power in comparison with standard solitons in a fiber with a dispersion equal to the average dispersion for the DM case (see Smith, Knox, Doran, Blow and Bennion [1996] and Gabitov and Turitsyn [1997]). It was also observed that four-wave mixing effects are significantly reduced (Kurtzke [1993]). As is well known, the appearance of solitons and MI are closely related problems. It is thus interesting to check the possibility of MI in fibers with periodic modulation of dispersion, for both weak and strong dispersion management.

The governing equation for this problem is

$$iu_z + d(z)u_{tt} + |u|^2u = 0, \quad (3.19)$$

where $d(z)$ is a periodic function. We start with the case of weak dispersion management, $d = d_0 + d_1(z)$, $d_1 \ll d_0$, where d_0 is the dispersion coefficient averaged over time. The stationary solution of eq. (3.19) is $u = A \exp(iA^2z)$. To perform the stability analysis we add a small spatio-temporal perturbation $\psi(z, t)$ to this solution, as we did in eq. (3.3). Substituting $\psi(z, t)$ in the form $\psi = a \exp(i\Omega t) + b^* \exp(-i\Omega t)$ we obtain the set of equations

$$ia_z = -\Omega^2 d(z)a - A^2(a + b), \quad (3.20)$$

$$ib_z = \Omega^2 d(z)b + A^2(a + b), \quad (3.21)$$

which can easily be reduced to an equation for the amplitude $a(z)$:

$$a_{zz} + q^2 [1 + \tilde{\alpha}_1 d_1(z) + \tilde{\alpha}_2 d_1^2(z) - i\tilde{\gamma} d_{1z}(z)] a = 0, \quad (3.22)$$

with the coefficients

$$q^2 = \frac{\Omega^2}{2\tilde{\gamma}}, \quad \tilde{\alpha}_1 = 4(\Omega^2 d_0 + A^2)\tilde{\gamma}, \quad \tilde{\alpha}_2 = 2\Omega^2\tilde{\gamma}, \quad \tilde{\gamma} = \frac{1}{\frac{1}{2}\Omega^2 + 4A^2}. \quad (3.23)$$

Because $d_1(z)$ is an arbitrary function it is not possible in general to solve eq. (3.22) analytically. Results can be obtained for particular choices of $d_1(z)$:

periodical modulations (Abdullaev, Darmanyany, Kobayakov and Lederer [1996], Smith and Doran [1996]) and stepwise dispersion-management (Bronski and Kutz [1996]). In this section we assume the dispersion is periodically modulated, viz. $d_1(z) = d_p \cos(k_p z)$. Then we can rewrite eq. (3.22) as

$$a_{zz} + Q^2 [1 + \alpha_1 \cos(k_p z) + \alpha_2 \cos(k_p z) + i\gamma \sin(k_p z)] a = 0, \quad (3.24)$$

with the new coefficients

$$Q^2 = q^2 \chi, \quad \alpha_1 = \frac{\tilde{\alpha}_1 d_p}{\chi}, \quad \alpha_2 = \frac{\tilde{\alpha}_2 d_p^2}{2\chi}, \quad \gamma = k_p d_p \tilde{\gamma}, \quad \chi = 1 + \frac{\tilde{\alpha}_2 d_p^2}{2}. \quad (3.25)$$

Equation (3.24) is the generalized Mathieu equation. For small $d_p \ll 1$ the standard perturbation method can be applied (Landau and Lifshitz [1973]). In doing so we find that the domain of MI is reduced relative to a fiber with constant anomalous dispersion.

In addition to this change, parametric resonance gives rise to new domains defined by $\frac{1}{2} m k_p = Q$, $m = 1, 2, 3, \dots$. The first parametric resonance corresponds to

$$Q = \frac{1}{2} k_p + \varepsilon_1, \quad (3.26)$$

where ε_1 denotes the detuning from the resonance. The increment of the instability λ_1 of this first resonance is then given by

$$\lambda_1^2 = \frac{1}{16} q^2 (\alpha_1^2 - \gamma^2) - \varepsilon_1^2, \quad (3.27)$$

where we have neglected the terms proportional to α_2 , which yield higher-order corrections. From eq. (3.27) we can easily see that the maximum increment of instability and the width of the resonance ε_{1m} coincide, amounting to

$$\lambda_{1 \max} = |\varepsilon_{1m}| = \frac{1}{2} d_p q \tilde{\gamma} A^2. \quad (3.28)$$

The center frequency $\Omega_{\text{res } 1}$ of this resonance is obtained upon substitution of $q = q(Q)$ from eq. (3.23) into eq. (3.26) as

$$\Omega_{\text{res } 1}^2 = \sqrt{4A^4 + k_p^2} - 2d_0 A^2, \quad (3.29)$$

and the width $\Delta\Omega_1$ is determined by

$$\Delta\Omega_1 = \frac{d_p A^2 \Omega_{\text{res } 1}}{2(\Omega_{\text{res } 1}^2 + 2d_0 A^2)}. \quad (3.30)$$

The first conclusion to be drawn from eq. (3.29) is that the oscillations of the dispersion entail MI for the case of normal dispersion for *any* $\Omega > 0$. Secondly,

for the anomalous dispersion a new domain of MI (parametric instability region) occurs for $\Omega > \Omega_{\text{MI}}$. If the period of the dispersion variations is small ($k_p^2 \gg 2A^2$), we obtain $\Omega_{\text{res}1} = \sqrt{k_p}$ for the location of the resonance.

The second parametric resonance appears at $Q = k_p + \varepsilon_2$, with the corresponding resonance frequency

$$\Omega_{\text{res}2}^2 = 2(\sqrt{A^2 + k_p^2} - d_0 A^2). \quad (3.31)$$

It can be shown that the instability domain is asymmetric with respect to the central frequency (Abdullaev, Darmanyan, Kobayakov and Lederer [1996]).

The instability of soliton sidebands during soliton propagation in a fiber with periodic dispersion has the same origin as the MI resonances (Abdullaev, Caputo and Flytzanis [1994]).

The analysis of MI in fibers with strong dispersion management (Smith and Doran [1996]) shows that the fundamental MI region is changed. This differs from the case of periodic variations of the amplification considered in the previous section. Also, sideband formation is suppressed under strong dispersion management. Note that in case of periodic variation of amplification the spectral component couples with one spectral sideband, while in DM even one harmonic modulation of $d(z)$ generates a complete set of sidebands. The MI induced by the periodic variation of dispersion has been experimentally observed in a long-distance transmission system by Shiraki, Omae and Horiguchi [1998].

3.3. MI in a fiber Bragg grating

In this subsection we consider the MI of electromagnetic waves in a cubic nonlinear dielectric medium with periodically modulated dielectric constant, with the period of modulation close to the optical wavelength. A typical example of such a medium is an optical fiber with Bragg grating. The governing equation is

$$E_{zz} - \frac{\epsilon(z)}{c^2} E_{tt} = \mu_0 P_{tt}^{\text{NL}}, \quad (3.32)$$

where $\epsilon(z) = \bar{n}^2 + 2\bar{\epsilon} \cos(2k_0 z)$, $k_0 = 2\pi/d_0$, and d_0 is the period of the modulations of the medium. The electric field has the form

$$E(\mathbf{r}, t) = \xi(\mathbf{r}) \exp(-i\omega t) + \text{c.c.}$$

The nonlinear response is

$$P^{\text{NL}} = \epsilon_0 (A(\xi \cdot \xi^*) \xi \exp(-i\omega t) + \frac{1}{2} B(\xi \cdot \xi) \xi^* \exp(-i\omega t) + \text{c.c.})$$

Periodic variations of both a linear and a nonlinear index of refraction can be produced in fibers, e.g., by corrugating the core-cladding structure. When

the period of the variations is of the order of the optical wavelength the Bragg reflection is large. As a result, the amplitude of the reflected wave is of the same order as that of the forward-going wave. One of the possible approaches to the study of MI is to use coupled-mode theory, i.e. to consider counter-propagating waves. According to this approach we can look for a solution of the form

$$E(z, t) = E_+(z, t) \exp[-i(\omega_0 t - k_0 z)] + E_-(z, t) \exp[-i(\omega_0 t + k_0 z)] + \text{c. c.}, \quad (3.33)$$

where E_{\pm} are the envelopes of the forward- and back-propagating waves, respectively. The coupled-mode equations are (Winful and Cooperman [1982], De Sterke and Sipe [1990], Acevcs [2000])

$$i \left(\partial_z + \frac{\bar{n}}{c} \partial_t \right) E_+ + \kappa E_- + \Gamma_s (|E_+|^2 + 2|E_-|^2) E_+ = 0, \quad (3.34)$$

$$i \left(-\partial_z + \frac{\bar{n}}{c} \partial_t \right) E_- + \kappa E_+ + \Gamma_s (|E_-|^2 + 2|E_+|^2) E_- = 0, \quad (3.35)$$

where

$$\Gamma_s = \frac{\omega^2}{2\bar{n}c} \left(A + \frac{B}{2} \right), \quad \kappa = \frac{\omega_0 \bar{\epsilon}}{2\bar{n}c}.$$

The cw solution is

$$E_+ = \frac{a}{\sqrt{1+f^2}} \exp[i(Qz - \Omega t)], \quad E_- = \frac{af}{\sqrt{1+f^2}} \exp[i(Qz - \Omega t)], \quad (3.36)$$

where

$$\Omega = \frac{1}{2} \kappa (f^{-1} + f) - \frac{3}{2} \Gamma a^2, \quad Q = -\frac{1}{2} \kappa (f^{-1} + f) - \frac{1}{2} \Gamma a^2 \frac{1-f^2}{1+f^2}.$$

It follows that the parameter a is related to the power of the grating through $a^2 = |E_+|^2 + |E_-|^2$. The meaning of the parameter f can be established by considering the linear limit ($a \rightarrow 0$). We see that the case $f < 0$ corresponds to the upper (positive) branch of the dispersive curve and $f > 0$ corresponds to the lower (negative) branch.

Let us consider the stability of these waves against small perturbations, following the work by De Sterke [1998]:

$$E_{\pm} = (a_{\pm} + \epsilon_{\pm}(z, t)) \exp[i(Qz - \Omega t)]. \quad (3.37)$$

Substituting eq. (3.37) into eq. (3.34) and neglecting terms of order ϵ^2 , we get the equations for the small perturbations ϵ_{\pm} :

$$\begin{aligned} i(\partial_t + \partial_z) \epsilon_+ + \kappa \epsilon_- - \kappa f \epsilon_+ + G [(\epsilon_+ + \epsilon_+^*) + 2f(\epsilon_- + \epsilon_-^*)] &= 0, \\ i(\partial_t - \partial_z) \epsilon_- + \kappa \epsilon_+ - \kappa f^{-1} \epsilon_- + G [2f(\epsilon_+ + \epsilon_+^*) + f^2(\epsilon_- + \epsilon_-^*)] &= 0, \end{aligned} \quad (3.38)$$

where $G = \Gamma a^2 / (1 + f^2)$. One can look for a solution of the form

$$\epsilon_{\pm} = A_{\pm} \cos(qz - \omega t) + iB_{\pm} \sin(qz - \omega t). \quad (3.39)$$

The solvability condition gives the characteristic equation

$$\begin{aligned} (\omega^2 - q^2)^2 - 2\kappa^2(\omega^2 - q^2) - \kappa^2 f^2(\omega + q)^2 - \kappa^2 f^{-2}(\omega - q)^2 \\ + 4\kappa G f(3q^2 - \omega^2) = 0. \end{aligned} \quad (3.40)$$

The coefficients of this equation are real. Thus the complex conjugate roots correspond to the MI of the cw solution. For the particular case $f = \pm 1$, where $f = 1$ and $f = -1$ correspond to the top and the bottom of the photonic band gap, respectively, eq. (3.40) can be solved analytically.

(a) Top of the photonic band gap, $f = 1$. This case corresponds to anomalous dispersion and so we can expect the existence of MI. Indeed, the dispersion relation is

$$\omega^2 = q^2 + 2\kappa(\kappa - G) \pm \sqrt{\kappa^2(\kappa - G)^2 + \kappa q^2(\kappa + 2G)}. \quad (3.41)$$

We have MI of cw for the wavenumbers between $-\sqrt{12\kappa G}$ and $+\sqrt{12\kappa G}$. The maximal growth rate is obtained at the wavenumber

$$q_m = \sqrt{3\kappa G \frac{2\kappa + G}{\kappa + 2G}}. \quad (3.42)$$

(b) Bottom of the photonic band gap, $f = -1$ (normal dispersion). Then eq. (3.40) transforms to

$$\omega^2 = q^2 + 2\kappa(\kappa + G) \pm 2\sqrt{\kappa^2(\kappa + G)^2 + \kappa q^2(\kappa - 2G)}. \quad (3.43)$$

Analysis of this equation shows that the instability of cw exists only for

$$|q| > (\kappa + G)\sqrt{\frac{\kappa}{2G - \kappa}}.$$

For details we refer to the work by De Sterke [1998].

3.4. MI in nonlinear media with periodic potential

In this section we study the problem of MI in the NLS equation with a periodic potential $V(x+a) = V(x)$:

$$iu_t + du_{xx} + V(x)u + \chi|u|^2u = 0. \quad (3.44)$$

This problem appears in the investigation of pulse propagation with a periodic phase modulation in fibers, using lumped modulators in the time domain (see the book by Hasegawa and Kodama [1995]). Another example of a physical system described by eq. (3.44) is the Bose–Einstein condensate (BEC) in an optical lattice. We remind that in fibers x and t are interchanged, so the potential V is periodic in time.

One of the ways to study the MI in such a system is the reduction of this equation to an effective NLS equation with constant coefficients (Pötting, Meystre and Wright [2000], Konotop and Salerno [2002]). Let us consider a periodic potential of the form $V(x) = V_0 \cos^2(k_0x)$. Such a form of the potential applies for the BEC condensate in an optical lattice. The derivation procedure consists in using the linear eigenfunctions $\phi_{n,k}$ of eq. (3.44):

$$d \frac{d^2 \phi_{n,k}}{dx^2} + V_0 \cos^2(k_0x) \phi_{n,k} = E_{n,k} \phi_{n,k}. \quad (3.45)$$

Let us consider the wave packet for a given band index n and wavenumbers distributed in an interval of length Δk around the carrier k_0 . The parameters of

the wave packet are assumed to vary slowly on the scale of modulations $2\pi/k_0$. Then the field function can be written in the form

$$u(x, t) = U(x, t) \phi_{n, k_0} \exp(-iE_{n, k_0} t). \quad (3.46)$$

Substituting this approximation into eq. (3.44) we obtain the equation for the slowly varying envelope:

$$i(U_t + v_g U_x) + \frac{1}{2m_{\text{eff}}} U_{xx} + \chi |U|^2 U = 0, \quad (3.47)$$

where

$$\frac{1}{m_{\text{eff}}} = \frac{\partial^2 E_{n, k}}{\partial k^2} (k = k_0), \quad v_g = \frac{\partial E_{n, k}}{\partial k} (k = k_0).$$

Here m_{eff} is the effective mass of the Bloch state and v_g is the group velocity. Depending on the choice of the sign m_{eff} which is the curvature of the energy band (i.e. taking parameters near the bottom or the top of the Bloch zone) we can have stable or unstable cw solutions. This approach explains, for example, why dark (bright) solitons can be created in periodic media with a focusing (defocusing) Kerr nonlinearity.

3.5. MI in birefringent fibers with periodic dispersion

Another problem worth studying here is the propagation of two polarized electromagnetic waves in a periodic transmission line with variable dispersion $d(z)$. The governing equation is a system of two coupled modified NLS equations:

$$iu_z + d(z)u_{tt} + \gamma(|u|^2 + \alpha|v|^2)u = 0, \quad (3.48)$$

$$iv_z + d(z)v_{tt} + \gamma(\alpha|u|^2 + |v|^2)v = 0, \quad (3.49)$$

where $\alpha = 1$ for orthogonally polarized waves. For a birefringent fiber, $\alpha \approx \frac{2}{3}$ (Agrawal [1995], Georges [1998]). The system has the nonlinear plane-wave solutions

$$u_0 = A \exp[i\gamma(A^2 + \alpha B^2)z], \quad v_0 = B \exp[i\gamma(B^2 + \alpha A^2)z]. \quad (3.50)$$

We perform the linear stability analysis, as described in previous sections, following the work by Abdullaev and Garnier [1999]. Separating corrections $\psi_1 = a + ib$, $\psi_2 = e + if$ we get the system

$$a_z = d(z) \Omega^2 b, \quad (3.51)$$

$$b_z = -d(z) \Omega^2 a + 2\gamma A(Aa + \alpha Be), \quad (3.52)$$

$$e_z = d(z) \Omega^2 f, \quad (3.53)$$

$$f_z = -d(z) \Omega^2 e + 2\gamma B(Be + \alpha Aa). \quad (3.54)$$

Throughout this section we shall consider the particular case $A = B$ which simplifies the algebra. The MI gain is defined as the maximal exponential growth of a^2 , b^2 , e^2 and f^2 .

Let us consider the particular case where $d(z)$ is stepwise constant and takes two different values d_1 and d_2 at regularly spaced intervals with lengths L_1 and L_2 . The system is periodic with period $L = L_1 + L_2$, i.e.

$$d(x) = \begin{cases} d_1 & \text{if } x \in [nL, nL + L_1), & n \in \mathbb{N}, \\ d_2 & \text{if } x \in [nL + L_1, (n+1)L), & n \in \mathbb{N}. \end{cases}$$

Equations (3.51)-(3.54) can be solved analytically for this form of $d(z)$.

The eigenvalues have the following forms:

$$\lambda_1^\pm = a^\pm + \sqrt{(a^\pm)^2 - 1}, \quad \lambda_2^\pm = a^\pm - \sqrt{(a^\pm)^2 - 1}, \quad (3.55)$$

where

$$a^\pm := \cos(k_2^\pm L_2) \cos(k_1^\pm L_1) - \frac{1}{2}(r^\pm + r^{\pm-1}) \sin(k_2^\pm L_2) \sin(k_1^\pm L_1), \quad (3.56)$$

$$r^\pm := \frac{k_1^\pm d_2}{k_2^\pm d_1} \quad (3.57)$$

with

$$k_j^\pm = \sqrt{\beta_j \Omega^2 (\beta_j \Omega^2 - l^{\pm-1})}, \quad l^\pm = \frac{1}{2\gamma A^2 (1 \pm \alpha)}.$$

Note that a^\pm are always real-valued, as can be checked by simple algebra using the fact that k_j^\pm is either real-valued or purely imaginary.

Two cases are possible:

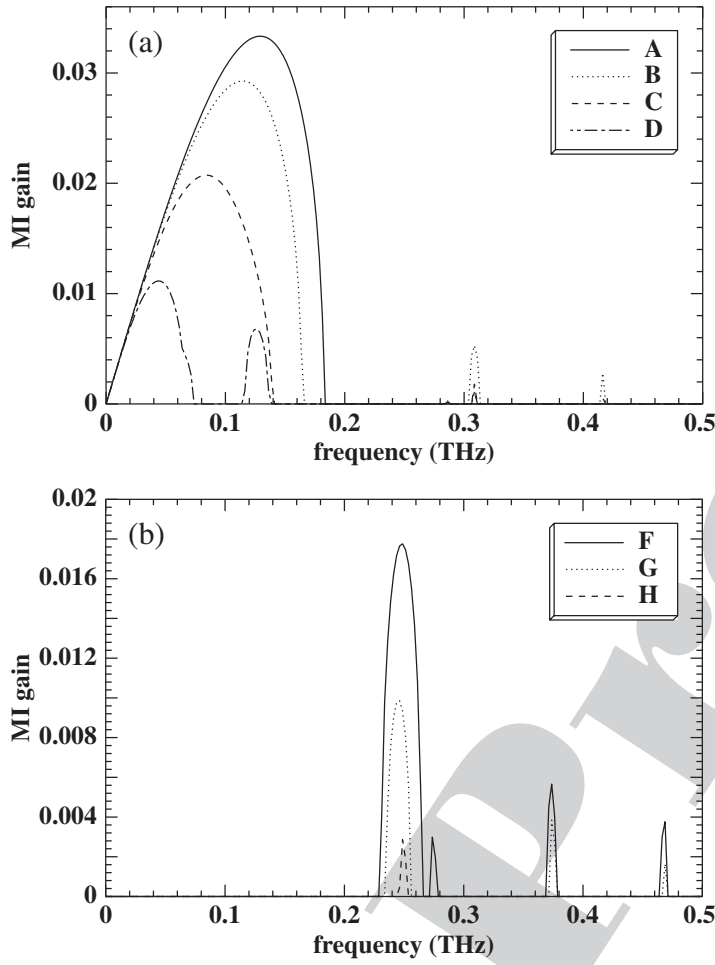


Fig. 2. (a) MI gain per unit length (in km) versus modulation frequency Ω (in THz) for $\gamma = 2 \text{ W}^{-1} \text{ km}^{-1}$, $L_1 = L_2 = 20 \text{ km}$, $P_0 = A^2 = 5 \text{ mW}$, and $\alpha = \frac{2}{3}$. Curve A corresponds to the standard anomalous dispersion $\beta_1 = \beta_2 = 1 \text{ ps}^2 \text{ km}^{-1}$. Curves B–D all have the same average anomalous dispersion $\bar{\beta} = (L_1\beta_1 + L_2\beta_2)/(L_1 + L_2) = 1 \text{ ps}^2 \text{ km}^{-1}$, but increasing dispersion management; B corresponds to $\beta_1 = 4$, $\beta_2 = -2 \text{ ps}^2 \text{ km}^{-1}$, C corresponds to $\beta_1 = 8$, $\beta_2 = -6 \text{ ps}^2 \text{ km}^{-1}$, and D corresponds to $\beta_1 = 16$, $\beta_2 = -15 \text{ ps}^2 \text{ km}^{-1}$. (b) Same as (a), for average normal dispersion $\bar{\beta} = -1 \text{ ps}^2 \text{ km}^{-1}$. F corresponds to $\beta_1 = -3$, $\beta_2 = 1 \text{ ps}^2 \text{ km}^{-1}$, G corresponds to $\beta_1 = -4$, $\beta_2 = 2 \text{ ps}^2 \text{ km}^{-1}$, and H corresponds to $\beta_1 = -8$, $\beta_2 = 6 \text{ ps}^2 \text{ km}^{-1}$.

- (i) If $a^{\pm 2} > 1$, then the eigenvalues λ_1^{\pm} and λ_2^{\pm} are real-valued and strictly different. Since the product $\lambda_1^{\pm} \lambda_2^{\pm}$ is equal to 1, at least one of the eigenvalues has a modulus larger than 1.

(ii) If $a^{\pm 2} \leq 1$, then, writing $b^{\pm} = \sqrt{1 - a^{\pm 2}}$, the eigenvalues are given by $\lambda_1^{\pm} = a^{\pm} + ib^{\pm}$ and $\lambda_2^{\pm} = a^{\pm} - ib^{\pm}$.

Thus there is stability if and only if $a^{-2} - 1$ and $a^{+2} - 1$ are non-positive-valued; otherwise the exponential gain is

$$G = \frac{2}{L} \max\left(\left|\ln[|a^+| + \sqrt{a^{+2} - 1}]\right|, \left|\ln[|a^-| + \sqrt{a^{-2} - 1}]\right|\right). \quad (3.58)$$

This equation reads as a closed-form expression which allows us to plot $G(\Omega)$ as a function of Ω for a given set of parameters $(\beta_1, \beta_2, L_1, L_2, \alpha, A)$.

For the case $L_1, L_2 \ll l^+, l^-$ we get that the resonant frequencies are

$$\Omega_p^{\pm 2} = \frac{\pi p}{|\beta|L} + \frac{1}{2\beta l^{\pm}}. \quad (3.59)$$

The resulting theoretical resonant peaks (fig. 2a) should be around $\Omega_1^+ \sim 0.31$, $\Omega_1^- \sim 0.29$, $\Omega_2^+ \sim 0.42$, $\Omega_2^- \sim 0.40$, $\Omega_3^+ \sim 0.50$, $\Omega_3^- \sim 0.49$ (in THz). These values agree well with the exact plot of the MI gain in fig. 2a. For fig. 2b the theoretical resonant peaks are predicted as $\Omega_1^+ \sim 0.25$, $\Omega_1^- \sim 0.275$, $\Omega_2^+ \sim 0.375$, $\Omega_2^- \sim 0.39$, $\Omega_3^+ \sim 0.47$, $\Omega_3^- \sim 0.48$ (in THz).

Figure 2a corresponds to the case of birefringent fibers with an average anomalous dispersion, when $\alpha = \frac{2}{3}$. We have considered the case when $\gamma = 2 \text{ W}^{-1} \text{ km}^{-1}$, $L_1 = L_2 = 20 \text{ km}$, $P_0 = A^2 = 5 \text{ mW}$. In these conditions the characteristic wavelengths are $l^+ = 30 \text{ km}$ and $l^- = 150 \text{ km}$. It appears that the central peak gain is progressively reduced as the strength of the dispersion management increases, and so are the resonant sidebands. For more details see Abdullaev and Garnier [1999].

Figure 2b corresponds to the case of birefringent fibers with an average *normal* dispersion, when $\alpha = \frac{2}{3}$. Although there is no MI gain in the uniform case $\beta = -1$, some new sidebands appear when the dispersion management is not zero, but these sidebands tend to disappear for strong dispersion management.

3.6. MI in fibers with periodic birefringence

In polarization-preserving birefringent optical fibers, two distinct forms of modulational instability occur: cross-phase modulational instability (Berkhoer and Zakharov [1970], Agrawal [1987]) and polarization modulational instability (PMI, Wabnitz [1988]). The periodic variations of birefringence change the phase-matching condition for the latter case, and as a result, sideband instability can occur for PMI.

Following the work by Murdoch, Leonhardt, Harvey and Kennedy [1997], we consider a weakly birefringent fiber with periodically varying birefringence. The variation can be achieved, for example, by wrapping the fiber between two spools. The resulting periodic variation is of the form

$$\delta\beta(z) = \begin{cases} 0, & m(l_1 + l_2) < z < m(l_1 + l_2) + l_1, \\ \delta\beta, & m(l_1 + l_2) + l_1 < z < (m + 1)(l_1 + l_2), \end{cases} \quad (3.60)$$

where $\delta\beta = k_x - k_y$, and k_x and k_y are the wavenumbers of the principal polarizations. The electric field is

$$\mathbf{E}(\mathbf{r}, t) = U(\mathbf{r}) \{ \mathbf{x}A_x(z, t) \exp[i(kz - \omega_0 t)] + \mathbf{y}A_y(z, t) \exp[i(kz - \omega_0 t)] \} + \text{c.c.}$$

Here $U(\mathbf{r})$ is the transverse-mode function. Using a standard procedure for averaging over transverse modes, we obtain the system of equations for the envelopes of waves in different polarizations:

$$iA_{x,z} - [\alpha(z) - \frac{1}{2}\delta\beta(z)] A_x - \frac{1}{2}\beta_2 A_{x,tt} + R(|A_x|^2 + \frac{2}{3}|A_y|^2) A_x + \frac{1}{3}RA_x^* A_y^2 = 0, \quad (3.61)$$

$$iA_{y,z} - [\alpha(z) - \frac{1}{2}\delta\beta(z)] A_y - \frac{1}{2}\beta_2 A_{y,tt} + R(|A_y|^2 + \frac{2}{3}|A_x|^2) A_y + \frac{1}{3}RA_y^* A_x^2 = 0, \quad (3.62)$$

where $\alpha(z) = k - \frac{1}{2}(k_x + k_y)$ in the birefringent section and $\alpha(z) = 0$ in the nonbirefringent section, $A_{x,y}$ are slowly varying envelopes along the birefringent axis, $R = n_2\omega_0/(cA_{\text{eff}})$, with A_{eff} the effective fiber core area, and n_2 is the nonlinear part of the refractive index.

Below we study the stability of the steady-state solutions

$$A_x = \sqrt{P} \exp(i\phi), \quad A_y = 0, \quad \phi = RPz - \int_0^z (\alpha - \frac{1}{2}\delta\beta) dz'. \quad (3.63)$$

To perform the linear stability analysis, let us look for the solutions of the form

$$A_x = A_x^0 + \delta A(z, t), \quad A_y = b(z, t) e^{i\phi}, \quad \delta A, b \ll |A_x|. \quad (3.64)$$

From eqs. (3.61), (3.63) and (3.64) we get the equation for the small perturbation $b(z, t)$:

$$ib_z - \frac{1}{2}\beta_2 b_{tt} + \frac{1}{3}RP[b^* - b] - \delta\beta(z) b = 0. \quad (3.65)$$

The regions of MI can be determined explicitly, since the variations of the birefringence are piecewise (see eq. 3.60). The Floquet discriminant

defining $K(\Omega)$ can be calculated explicitly. The gain of MI is calculated as $g(\Omega) = 2\text{Im}[K(\Omega)]$, namely $\Delta(\Omega) = 2 \cos(K(\Omega)L)$. The stability region corresponds to $-2 < \Delta(\Omega) < 2$. The calculation of the discriminant gives

$$\begin{aligned} \Delta(\Omega) &= 2 \cos(k_1 l_1) \cos(k_2 l_2) - \frac{k_1^2 + k_2^2 - \delta\beta^2}{k_1 k_2} \sin(k_1 l_1) \sin(k_2 l_2) \\ &= 2 \cos[k_2(l_1 + l_2)], \end{aligned} \quad (3.66)$$

where

$$\begin{aligned} k_1^2 &= \frac{1}{2}\beta_2\Omega^2(\frac{1}{2}\beta_2\Omega^2 - \frac{2}{3}RP), \\ k_2^2 &= (\frac{1}{2}\beta_2\Omega^2 - \delta\beta)(\frac{1}{2}\beta_2\Omega^2 - \delta\beta - \frac{2}{3}RP). \end{aligned} \quad (3.67)$$

The values of the frequency shift of PMI sidebands can be approximated by the formula

$$\Omega_n = \sqrt{\frac{1}{\beta_2} \left(\frac{2\delta\beta l_2}{l_1 + l_2} + \frac{2}{3}RP + \frac{2n\pi}{l_1 + l_2} \right)}. \quad (3.68)$$

The analysis of the expression for the PMI gain spectrum (3.66) shows that a series of sidebands is generated. The typical experimental parameter values are: $\Delta n = n_x - n_y = 6.8 \times 10^{-6}$, $l_2 = 2.53$ cm, $R = 0.025$ m⁻¹ W⁻¹, $\beta_2 = 50$ ps² km⁻¹, $P = 700$ W. We obtain for the sideband with $n = 0$ and $l_1 = 0$ that the PMI gain is 11.5 m⁻¹ and the frequency shift is ~7 THz; with $l_1 = 10$ cm the gain is 8.5 m⁻¹.

Experimental results obtained by Murdoch, Leonhardt, Harvey and Kennedy [1997] confirm these predictions for the PMI sidebands.

3.7. MI in periodic quadratic nonlinear media

The next important example of a nonlinear physical system with periodically modulated parameters comprises quadratic nonlinear media with periodic inhomogeneities. In quadratic nonlinear media the main parameter defining wave interaction is the phase mismatch. Particular values of this parameter give the strongest interaction and mutual transformation of the FW and SH waves. Stable optical solitons can exist in these media at all dimensions, starkly different from the case of Kerr nonlinearity. On the other hand, the existence of the strong cascading limit permits the observation of many phenomena known from Kerr nonlinearity in the quadratic case. Periodic variation of the linear and nonlinear parameters of such a medium lead to compensation of the large phase mismatch

and as a consequence to the existence of new types of solitons. Experimentally, such modulations were realized using periodically poled Li_2NbO_3 (Fejer, Magel, Jundt and Byer [1992]) and GaAs/GaAlAs structures (Petrov [1996]). The influence of the periodic inhomogeneities on the MI in $\chi^{(2)}$ media has been studied by Corney and Bang [2001]. Below we follow this work.

Let us consider beam propagation in a quadratic medium having modulations of linear and nonlinear refraction indices with a period much longer than the optical period. In this case Bragg reflection can be neglected and we can write the system of equations for the envelopes of FW and SH propagating waves.

The governing equations for FW and SH waves propagating in periodic quadratic nonlinear 1D media are

$$\begin{aligned} iE_{1,Z} + \frac{1}{2}E_{1,XX} + \alpha_1 E_1 + \chi E_1^* E_2 \exp(i\beta Z) &= 0, \\ iE_{2,Z} + \frac{1}{4}E_{2,XX} + 2\alpha_2 E_2 + \chi E_1^2 \exp(-i\beta Z) &= 0. \end{aligned} \quad (3.69)$$

Here $E_i(X, Z)$ are the envelopes of the FW and SH waves. The coordinate X is measured in the input beam width X_0 , the coordinate Z in the diffraction length $L_d = k_1 X_0^2$; $\beta = \Delta k L_d$, where $\Delta k = k_2 - 2\beta_1$, $k_j = i\omega n_j$ is the phase mismatch. The normalized linear refractive index grating is $\alpha_j(Z) = L_d \omega \Delta n_j(Z)$, and the normalized nonlinear grating is $L_d \omega d_{\text{eff}}(Z)/(n_i c)$, where $d_{\text{eff}} = \frac{1}{2}\chi^{(2)}$. The gratings α_j and χ_j are assumed to be periodic functions with period $2L_0 = 2\pi/|k_g|$, with k_g the spatial period of the grating. It is useful to study rescaled equations for new variables,

$$\begin{aligned} iw_z + \frac{1}{2}w_{xx} - rw + \chi' w^* v \exp(i\delta z) &= 0, \\ iv_z + \frac{1}{4}v_{xx} - \sigma v + \alpha' + \chi' w^2 \exp(-i\delta z) &= 0, \end{aligned} \quad (3.70)$$

where $w(x, z) = E_1 \exp(i\theta)$, $v(x, z) = E_2(X, Z) \exp(2i\theta + i\beta Z)$, $x = \sqrt{\eta}(X + \Omega Z)$, $z = \eta Z$, $\eta = |\Lambda + \Omega^2/2|$, and Λ and Ω are the longitudinal wavenumber offset and the transverse wavenumber respectively. The residual phase mismatch is $\tilde{\beta} = \beta - k_g$ and $\theta = \Lambda Z - \int \alpha_1(z) dz$. Here also $r = \text{sgn}(\Lambda + \frac{1}{2}\Omega^2)$, $\sigma = 2r - \beta'$.

To study this system it is useful to expand the rescaled gratings and fields in Fourier series, i.e.

$$\alpha' = \alpha' \sum_n g_n \exp(in\kappa z), \quad \chi' = \alpha'_0 + \alpha' \sum_n g_n \exp(in\kappa z) \quad (3.71)$$

and

$$w = \sum_n w_n(z, x) \exp(in\kappa z), \quad v = \sum_n v_n \exp(in\kappa z), \quad (3.72)$$

where $\kappa = k_g/\eta$, $\alpha' = 2(\alpha_2 - \alpha_1)/\eta$, and $g_n = 2s/(i\pi n)$, with $s = \text{sgn} \kappa$ for n odd, and $g_n = 0$ for n even.

The scales of the problems considered here are the diffraction length $L_d = \eta$, the coherence length $L_c = \pi/|\beta'|$, and the grating domain length $L_0 = \pi/|k_g|$. Typical values for the parameters are $k = 100$, $a' = d'_0 = 0$ in LiNbO₃, and $d'_0/d' = 4.6$, $d'/k = \frac{10}{46}$ in a GaAs/AlAs superstructure. The natural small parameter here is $\epsilon = L_0/L_d \ll 1$, which is satisfied for typical gratings. The harmonics $w_{n \neq 0}, v_{n \neq 0}$ are of order ϵ . We will assume effective phase matching. Then the residual mismatch is small, i.e. $|\beta'| \ll |k_g|$. Then by collecting the first-order terms in ϵ we can find the expressions for the harmonics as

$$\begin{aligned} w_{n \neq 0} &= \frac{(d'g_{n-1} + d'_0\delta_{n,1})w_0^*v_0}{n\kappa}, \\ v_{n \neq 0} &= \frac{d'g_n v_0 + (d'g_{n+1} + d'_0\delta_{n,-1})w_0^2}{n\kappa}. \end{aligned} \quad (3.73)$$

Using this result we can derive the averaged equations for $W, V = w_0, v_0$:

$$\begin{aligned} iW_z + \frac{1}{2}W_{xx} - rW + \rho W^* V + \gamma(|V|^2 - |W|^2)W &= 0, \\ iV_z + \frac{1}{4}V_{xx} - \sigma V + \rho W^2 + 2\gamma|W|^2V &= 0. \end{aligned} \quad (3.74)$$

For a square grating we have $\rho = 2is(d' - d'_0/\kappa)/\pi$, $\gamma = [d_0'^2 + d'^2(1 - 8/\pi^2)]/\kappa$.

Thus, from the analysis of the averaged equations we can conclude that the two principal effects of fast periodic modulations are the reduction of the effective quadratic interaction and the appearance of new (cubic) nonlinearities. The sign of the induced Kerr nonlinearity determines whether the MI gain is reduced or enhanced. Indeed, the defocusing effective Kerr nonlinearity stabilizes the background.

Applying the linear stability analysis as in § 2.2, we obtain the expression for the complex matrix \mathbf{M} :

$$\mathbf{M} = i \begin{pmatrix} a & b & c & d \\ -b & -a & -d & -c \\ 2c & 2d & g & 0 \\ -2d & -2c & 0 & -g \end{pmatrix}, \quad (3.75)$$

where $a = -\frac{1}{2}\Omega^2 - r + \gamma(|v_s|^2 - 2w_s^2)$, $b = \rho v_s - \gamma w_s^2$, $c = \rho w_s + \gamma v_s w_s$, $d = \gamma v_s w_s$, and $g = -\frac{1}{4}\Omega^2 - \sigma + 2\gamma w_s^2$.

For $r = 0$ and $r = 1$ all nondegenerate and nontrivial solutions are unstable. The result of numerical analysis for other regions can be found in the article by Corney and Bang [2001].

These results have been obtained in the framework of the averaged theory. The exact stability analysis involves the analysis of eigenvalues of the matrix of

the linear stability problem \mathbf{M} with periodic coefficients. Application of Floquet theory shows that the averaged theory accurately predicts the properties of the lower part of the MI spectrum. The analysis of the higher part of the spectrum necessitates the application of exact Floquet analysis.

§ 4. MI in random media

4.1. Origins of random fluctuations

All the results discussed in the previous sections were obtained in media where the characteristic parameters are either constants or periodic functions. In realistic fiber transmission links, the nonlinearity and the chromatic dispersion are not constant but can fluctuate stochastically around their mean values. The inhomogeneity of the medium may be induced by other propagating waves (Agrawal [1987]) or may be intrinsic to the medium (Kodama, Maruta and Hasegawa [1994]). As there are various physical reasons for the fluctuations of the fiber parameters, we may encounter fluctuations whose spectrum has components with short length scales (around meters) and long length scales (around kilometers).

Usually the short-scale perturbations originate from variations of the fiber parameters – such as core radius, fiber geometry or index of refraction – generated during the drawing process. They may also be induced by mechanical distortions of fibers in practical use, such as point-like pressure or twists. The correlation length of such fluctuations is less than 1 meter. Direct measurements of the chromatic dispersion at these scales are usually not feasible, but it can be calculated from measurements of the fiber parameters such as the fiber radius or the index difference. For instance, the standard deviation of the fiber radius is typically about $0.1 \mu\text{rad}$ ($\sim 1\%$ error). As a result, the standard deviation in the chromatic dispersion is about $0.1 \text{ ps}^2 \text{ km}^{-1}$. Similarly, the standard deviation of the relative index difference is about 0.02% , and the induced standard deviation in the chromatic dispersion is about $0.4 \text{ ps}^2 \text{ km}^{-1}$ (Kuwaki and Ohashi [1990]). Fluctuations in the nonlinear coefficient are also caused by variations of the core radius and geometry which slightly affect the transverse profile of the mode and the effective nonlinear coefficient.

Long-scale fluctuations can also arise in the drawing process, as a result of a slow drift of the operating parameters. They may also be induced by long-scale fluctuations of the environment of the fiber in practical use, such as temperature variations for fibers in the ground. The literature contains

many results of measurements for the longitudinal variations of the chromatic dispersion (see for instance Mollenauer, Mamyshev and Neubelt [1996]), since they involve fluctuations of the zero-dispersion wavelength which in turn leads to the degradation of the optical system performance (Karlsson [1998]). Typical standard deviations for the chromatic dispersion and the nonlinear coefficient are of the same order as those cited for the short-scale fluctuations, while the typical length scales are of the order of a kilometer or longer (Nakajima, Ohashi and Tateda [1997]).

The chromatic dispersion and the nonlinear coefficient are not the only parameters that can suffer from random modulations in real optical fibers. Single-mode fibers are actually bimodal because of birefringence (Kaminow [1981]). The details of the birefringence evolution along the fiber are not known, but it is usually assumed that the birefringence is locally linear and that the strength and the orientation of the birefringence vary randomly along the fiber with a typical length scale whose spectrum may have components from a few centimeters to hundreds of meters (Simon and Ulrich [1977], Rashleigh [1983]). More exactly, the birefringence is small in absolute values in communication fibers, with values of the order of $\Delta n/n \approx 10^{-7}$. The corresponding beat length is only about 10 meters, which is far smaller than the typical nonlinear and dispersive lengths of the order of a few hundreds of kilometers. This would involve dramatic distortion in communication systems, but fortunately the orientation of the birefringence is also randomly varying on a length scale of about 100 meters, which averages out the effect of birefringence to zero. The residual effect leads to pulse spreading, referred to as Polarization Mode Dispersion (PMD). The effects due to PMD accumulate along the length of an optical fiber, as do the effects due to chromatic dispersion and nonlinearity.

4.2. The random scalar case

4.2.1. Linear stability analysis

The evolution of the field in random fibers is governed by the NLS equation with random coefficients (Agrawal [1995]):

$$iu_z + \beta u_{tt} + \gamma |u|^2 u = 0, \quad (4.1)$$

where we used the standard dimensionless variables. γ is a nonlinear coefficient. The Group Velocity Dispersion (GVD) coefficient is $\beta > 0$ ($\beta < 0$) for anomalous

(normal) dispersion. Both coefficients fluctuate around their respective mean values γ_0 and β_0 so that they can be described as:

$$\gamma(z) = \gamma_0 (1 + m_\gamma(z)), \quad \beta(z) = \beta_0 (1 + m_\beta(z)), \quad (4.2)$$

where m_β and m_γ are stationary, zero-mean and random processes. A usual model for a random fiber is the random concatenation of different fiber sections whose coefficients have constant values (Mollenauer, Smith, Gordon and Menyuk [1989], Wai, Menyuk and Chen [1991]). Typically the lengths of these segments are of the order of 10–100 km, which is usually less than the dispersion distance $L_d = t_0^2/|\beta_0|$: with the pulse duration t_0 of the order of 10 ps and the mean GVD coefficient of the order of $0.1 \text{ ps}^2 \text{ km}^{-1}$ for most glass fibers, $L_d \approx 1000 \text{ km}$. A white-noise model is justified for such a configuration. However some fibers have values of GVD in the range $1\text{--}10 \text{ ps}^2 \text{ km}^{-1}$, so that $L_d \approx 10\text{--}100 \text{ km}$ becomes of the same order as the correlation length. A more elaborate model (colored noise) is then necessary.

Equation (4.1) has continuous-wave solutions

$$u(z, t) = \sqrt{P_0} \exp\left(iP_0 \int_0^z \gamma(z') dz'\right).$$

Their linear stability is determined by considering a perturbed solution of the form

$$u(z, t) = \left(\sqrt{P_0} + u_1(z, t)\right) \exp\left(i \int_0^z \gamma(z') dz' P_0\right). \quad (4.3)$$

By substituting eq. (4.3) into eq. (4.1), and retaining only the first-order terms, one obtains a linear equation for $u_1(z, t)$:

$$iu_{1z} + \beta u_{1tt} + 2\gamma P_0 \text{Re}(u_1) = 0. \quad (4.4)$$

Performing the Fourier transform $\hat{u}_1 = \int u_1 \exp(-i\omega t) dt$, and using the complex representation $\hat{u}_1 = \hat{u}_{1r} + i\hat{u}_{1i}$, one obtains a system for the Fourier components of the perturbation term:

$$\frac{d}{dz} \begin{pmatrix} \hat{u}_{1r} \\ \hat{u}_{1i} \end{pmatrix} = Y(z) \begin{pmatrix} \hat{u}_{1r} \\ \hat{u}_{1i} \end{pmatrix}, \quad (4.5)$$

$$Y(z) = \begin{pmatrix} 0 & \beta(z)\omega^2 \\ 2\gamma(z)P_0 - \beta(z)\omega^2 & 0 \end{pmatrix}. \quad (4.6)$$

The basic linearized equations remain unchanged with respect to the homogeneous case, but β and γ are now random processes having the consequence

that \hat{u}_1 is random as well. Because the explicit form of \hat{u}_1 cannot be found, stochastic analysis has to be applied for analyzing the stochastic differential equation (SDE) satisfied by \hat{u}_1 . There are basically two ways to analyze the solutions of a SDE. Either we can determine the moments up to any order to describe the statistical properties of the sideband amplitude \hat{u}_1 , or (which is more general) we can examine the probability density function of \hat{u}_1 . The probability density function satisfies a partial differential equation known as the Fokker–Planck equation, and any expectation value can be determined from it. However the solution of a Fokker–Planck equation is usually intricate and cannot be written in closed form. Furthermore we are not interested in the complete determination of the statistical distribution of the sideband amplitude, but only in the statistical distribution of the growth rate of the modulation. This growth rate is characterized by the Lyapunov exponents of the linear system (4.5). The sample MI gain is defined as the Lyapunov exponent which governs the exponential growth of the modulation:

$$G(\omega) := \lim_{z \rightarrow \infty} \frac{1}{z} \ln |\hat{u}_1(z, \omega)|^2. \quad (4.7)$$

Note that $G(\omega)$ could be random since β and γ are. So it should be relevant to study the mean and fluctuations of the MI gain. For this purpose we shall analyze the $2n$ th mean MI gain defined as the normalized Lyapunov exponent which governs the exponential growth of the n th moment of the intensity of the modulation:

$$G_{2n}(\omega) := \lim_{z \rightarrow \infty} \frac{1}{nz} \ln \langle |\hat{u}_1(z, \omega)|^{2n} \rangle, \quad (4.8)$$

where the angle brackets stand for the expectation with respect to the distribution of the process (m_γ, m_β) . Note that this is a generalization of the standard mean MI gain G_2 which characterizes the exponential growth of the mean intensity of the modulation. If the MI process were deterministic, then we would have $G_{2n}(\omega) = G_2(\omega)$ for every n , since $\ln |\hat{u}_1(z, \omega)|^{2n} = n \ln |\hat{u}_1(z, \omega)|^2$. But due to randomness this does not hold true since we cannot invert the nonlinear power function “ $|\cdot|^n$ ” and the linear statistical averaging “ $\langle \cdot \rangle$ ”. Actually, Jensen’s inequality establishes that, if $n \geq 1$, then $\langle |\hat{u}_1(z, \omega)|^{2n} \rangle \geq \langle |\hat{u}_1(z, \omega)|^2 \rangle^n$, and consequently $G_{2n}(\omega) \geq G_2(\omega)$. If $G_{2n} = G_2 = G$ we can claim that the exponential growth is deterministic, but if G_{2n} increases with n , it means that the MI process is fluctuating.

Note that random matrix products theory applies to the problem (4.5), which gives qualitative information on the Lyapunov exponents (see, for instance,

Theorem 4 of Baxendale and Khaminskii [1998]). In the following we present closed-form expressions for the Lyapunov exponents $G(\omega)$ and $G_{2n}(\omega)$ in the natural framework corresponding to telecommunication applications, where the noise level is low.

4.2.2. The moment equations

We now present the standard approach applied when the random processes m_β and m_γ can be considered as Gaussian white noise:

$$\langle m_\beta(x) m_\beta(y) \rangle = 2\sigma_\beta^2 \delta(x-y), \quad \langle m_\gamma(x) m_\gamma(y) \rangle = 2\sigma_\gamma^2 \delta(x-y).$$

This approach is valid as long as the correlation lengths of the random perturbations are shorter than the dispersion distance. The first and most natural step consists in considering the evolution of the expectations of the modulation amplitudes. The solutions coincide with the deterministic and homogeneous case, apart from the inclusion of an exponentially decaying damping term, which in turn involves a reduction of the MI gain. From this we may conclude that random fluctuations always give rise to a reduction of the MI gain for anomalous dispersion where high-frequency modulations are more effectively damped, and do not introduce any MI for normal dispersion. Actually the stochastic resonance responsible for the MI induced by the random fluctuations is not captured by the analysis of the first moments. The first moments of the modulations actually decay because of the uncertainty in phase. Consider a toy model where \hat{u}_1 satisfies the equation $\frac{d\hat{u}_1}{dz} = i\hat{u}_1 q(z)$, where q is a Gaussian white noise. A closed-form expression for the solution is $\hat{u}_1(z) = \hat{u}_1(0) \exp(iW(z))$, where $W(z) := \int_0^z q(z') dz'$ is a Brownian motion ($\langle W(z)^2 \rangle = 2\sigma^2 z$). The expectation thus decays exponentially with z : $\langle \hat{u}_1(z) \rangle = \hat{u}_1(0) \exp(-\sigma^2 z)$, while the modulus of \hat{u}_1 is constant. Therefore it is misleading to consider only the expectation of the modulation amplitude, and it is relevant and necessary to compute the growth of the modulation intensity given by second-order moments. The problem at hand is actually analogous to a harmonic oscillator with a randomly perturbed frequency $v_{zz} + \omega_0^2(1 + q(z))v = 0$, where q is a random process. The equations for the first moments obey a trivial dynamics. The stochastic parametric resonance is only observed from the second-order moments equations as shown by Klyatskin [1980].

4.2.3. The second-moment MI gain

We now analyze the behavior of the second moments $\langle \hat{u}_{1r}^2 \rangle$, $\langle \hat{u}_{1i}^2 \rangle$ and $\langle \hat{u}_{1r} \hat{u}_{1i} \rangle$ (the crossed moment $\langle \hat{u}_{1r} \hat{u}_{1i} \rangle$ is added so as to close the equations for the second

moments). Applying Itô's formula (Revuz and Yor [1991], p. 145) the evolution of the column vector of the second moments $X^{(2)} := (\langle \hat{u}_{1r}^2 \rangle, \langle \hat{u}_{1r} \hat{u}_{1i} \rangle, \langle \hat{u}_{1i}^2 \rangle)^T$ reads as a closed-form linear system:

$$\frac{dX^{(2)}}{dz} = \mathbf{M}^{(2)} X^{(2)},$$

$$\mathbf{M}^{(2)} = \begin{pmatrix} -2\beta_0^2 \omega^4 \sigma_\beta^2 & 2\beta_0 \omega^2 & 2\beta_0^2 \omega^4 \sigma_\beta^2 \sigma_\gamma^2 \\ 2\gamma_0 P_0 - \beta_0 \omega^2 & -4\beta_0^2 \omega^4 \sigma_\beta^2 & \beta_0 \omega^2 \\ 2\beta_0^2 \omega^4 \sigma_\beta^2 + 8\gamma_0^2 P_0^2 \sigma_\gamma^2 & 2(2\gamma_0 P_0 - \beta_0 \omega^2) & -2\beta_0^2 \omega^4 \sigma_\beta^2 \end{pmatrix}.$$

Instability arises if an eigenvalue of $\mathbf{M}^{(2)}$ has a positive real part, and the mean MI gain G_2 defined by (4.8) is the largest value of the real parts of the eigenvalues of $\mathbf{M}^{(2)}$. The matrix $\mathbf{M}^{(2)}$ has three eigenvalues whose complete expressions have been given by Garnier and Abdullaev [2000]. These general expressions coincide with the particular cases studied by Abdullaev, Darmanyan, Bischoff and Sørensen [1997] and Abdullaev, Darmanyan, Kobayakov and Lederer [1996]. We now present and discuss these formulas, where the cut-off frequency $\omega_c := \sqrt{2\gamma_0 P_0 / |\beta_0|}$ plays an important role.

In case of normal dispersion, $\beta_0 < 0$, two eigenvalues are negative while the last one is positive for every frequency ω , which proves that there is instability for all frequencies:

$$G_2(\omega) = \beta_0^2 \frac{\omega_c^4 \omega^2}{\omega_c^2 + \omega^2 + 4\beta_0^2 \omega^6 \sigma_\beta^4} (\sigma_\beta^2 + \sigma_\gamma^2).$$

The optimal frequency and corresponding MI peak are given by:

$$\omega_{2,\text{opt}}^2 = (8\beta_0^4 \omega_c^2 \sigma_\beta^4)^{-1/3}, \quad G_{2,\text{opt}} = \frac{\beta_0^2 \omega_c^4}{1 + 3(|\beta_0| \omega_c^2 \sigma_\beta^2)^{2/3}} (\sigma_\beta^2 + \sigma_\gamma^2).$$

Let us now consider the anomalous dispersion regime, $\beta_0 > 0$. In the standard stable region $\omega > \omega_c$, the gain is positive for every frequency:

$$G_2(\omega) = \beta_0^2 \frac{\omega^2 \omega_c^4}{\omega^2 - \omega_c^2} (\sigma_\beta^2 + \sigma_\gamma^2).$$

For the study of the standard unstable region $\omega < \omega_c$, we introduce the dimensionless parameter $\delta := \sigma_\gamma^2 / \sigma_\beta^2$. Two cases can be distinguished.

If $\delta \leq 1$, which means that randomness essentially originates from GVD fluctuations, then the gain is

$$G_2(\omega) = 2\beta_0\omega\sqrt{\omega_c^2 - \omega^2} + 4\beta_0^2\omega^2 \frac{(\omega^2 - \omega_{-, \delta}^2)(\omega^2 - \omega_{+, \delta}^2)}{\omega_c^2 - \omega^2} \sigma_\beta^2,$$

where the two characteristic frequencies $\omega_{-, \delta}$ and $\omega_{+, \delta}$ are defined by

$$\omega_{-, \delta}^2 := \frac{2 - \sqrt{2(1 - \delta)}}{4} \omega_c^2, \quad \omega_{+, \delta}^2 := \frac{2 + \sqrt{2(1 - \delta)}}{4} \omega_c^2.$$

This shows that the random dispersion increases instability for $\omega \in (0, \omega_{-, \delta})$ and $\omega \in (\omega_{+, \delta}, \omega_c)$, and decreases it for $\omega \in (\omega_{-, \delta}, \omega_{+, \delta})$. The optimal frequency $\omega_{2, \text{opt}}$ is lower than the homogeneous optimal frequency $\omega_c/\sqrt{2}$, and the corresponding MI peak is *reduced*:

$$\omega_{2, \text{opt}}^2 = \frac{1}{2}\omega_c^2 - \frac{1}{2}\beta_0\omega_c^4(\sigma_\beta^2 - \sigma_\gamma^2), \quad G_{2, \text{opt}} = \beta_0\omega_c^2 - \frac{1}{2}\beta_0^2\omega_c^4(\sigma_\beta^2 - \sigma_\gamma^2). \quad (4.9)$$

If $\delta > 1$, which means that randomness essentially originates from fluctuations of the nonlinear coefficient, then the gain is:

$$G_2(\omega) = 2\beta_0\omega\sqrt{\omega_c^2 - \omega^2} + \beta_0^2\omega^2 \frac{(2\omega^2 - \omega_c^2)^2 + \frac{1}{2}(\delta - 1)\omega_c^4}{\omega_c^2 - \omega^2} \sigma_\beta^2,$$

which shows that the random nonlinearity makes instability increase for all frequencies $\omega \in (0, \omega_c)$. In particular the MI peak obtained at $\omega_{2, \text{opt}}$ is *enhanced* and given by eq. (4.9).

4.2.4. Higher-order moments

The results derived in the previous subsection give accurate expressions for the second-moment MI gain G_2 , but the relationship with the sample MI gain G is not obvious. Further it may seem arbitrary to characterize the stability of the continuous wave through the analysis of the second moment of the modulation \hat{u}_1 . In this subsection we present a study of the exponential growth of higher-order moments of \hat{u}_1 so as to get a picture of the fluctuations of the exponential growth of \hat{u}_1 . Let n be an integer and $X^{(2n)}$ be the $(2n + 1)$ -dimensional row

vector of the $2n$ th moments of the modulation: $X_j^{(2n)} := \langle \hat{u}_{1r}^{2n-j} \hat{u}_{1i}^j \rangle, j = 0, \dots, 2n$.

Applying Itô's formula establishes that the vector $X^{(2n)}$ satisfies

$$\frac{dX^{(2n)}}{dz} = \mathbf{M}^{(2n)} X^{(2n)},$$

where $\mathbf{M}^{(2n)}$ is a $(2n+1) \times (2n+1)$ matrix

$$\mathbf{M}^{(2n)} = (\beta_0 \omega^2 - 2\gamma_0 P_0) \mathbf{A}^{(2n)} - \beta_0 \omega^2 \mathbf{B}^{(2n)} + \beta_0^4 \omega^4 \sigma_\beta^2 \mathbf{C}^{(2n)} + 4\gamma_0^2 P_0^2 \sigma_\gamma^2 \mathbf{D}^{(2n)}.$$

The matrices $\mathbf{A}^{(2n)}$, $\mathbf{B}^{(2n)}$, $\mathbf{C}^{(2n)}$ and $\mathbf{D}^{(2n)}$ are null except for the following elements: $A_{j,j+1}^{(2n)} = 2n - j$, $B_{j,j-1}^{(2n)} = j$, $C_{j,j}^{(2n)} = -2n - 4nj + 2j^2$, $C_{j,j-2}^{(2n)} = j(j-1)$, $C_{j,j+2}^{(2n)} = (2n-j)(2n-j-1)$, and $D_{j,j-2}^{(2n)} = j(j-1)$. In this framework $nG_{2n}(\omega)$ is equal to the maximum of the real parts of the roots of the characteristic polynomial of the matrix $\mathbf{M}^{(2n)}$ whose degree is $2n+1$. This implies that the derivation of a closed-form expression for $G_{2n}(\omega)$ for any $n \geq 2$ is quite intricate, but it can be carried out numerically. Figures 3–5 display the MI gains G_{2n} for different values of n , σ_β and σ_γ , and compare them with full numerical simulations. As a model for the random processes m_β and m_γ in the simulations we have chosen step-wise constant functions which take independent and random values in $\{-\sigma, \sigma\}$ over elementary intervals with lengths l . This configuration can be approximated by a white-noise model with $\sigma_\beta^2 = \sigma_\gamma^2 = \frac{1}{2} \sigma^2 l$. Comments on the figures, as well as further theoretical investigations, will be given in the next subsection.

4.2.5. The sample and mean growth exponents

Figures 3–5 show that the moments of the modulation \hat{u}_1 grow with different exponential rates. This provides evidence that the behavior of the modulation is not deterministic but exhibits strong random fluctuations. It should thus be relevant to study the complete distribution of the MI gain, and not only the first moments. Furthermore, only the case of white noise has been addressed in the previous subsection, but it should be relevant also to consider general colored noise and to study the influence of the power spectrum of the noise. The answers to these questions can be found by applying elaborate tools of stochastic analysis that compute the expansion of the Lyapunov exponents of randomly perturbed linear systems. Garnier and Abdullaev [2000] have applied this method to compute the statistical distributions of the Lyapunov exponents of the system (4.5). A striking point is that the statistical distribution of the modulation intensity can be expressed in terms of log-normal statistics. The

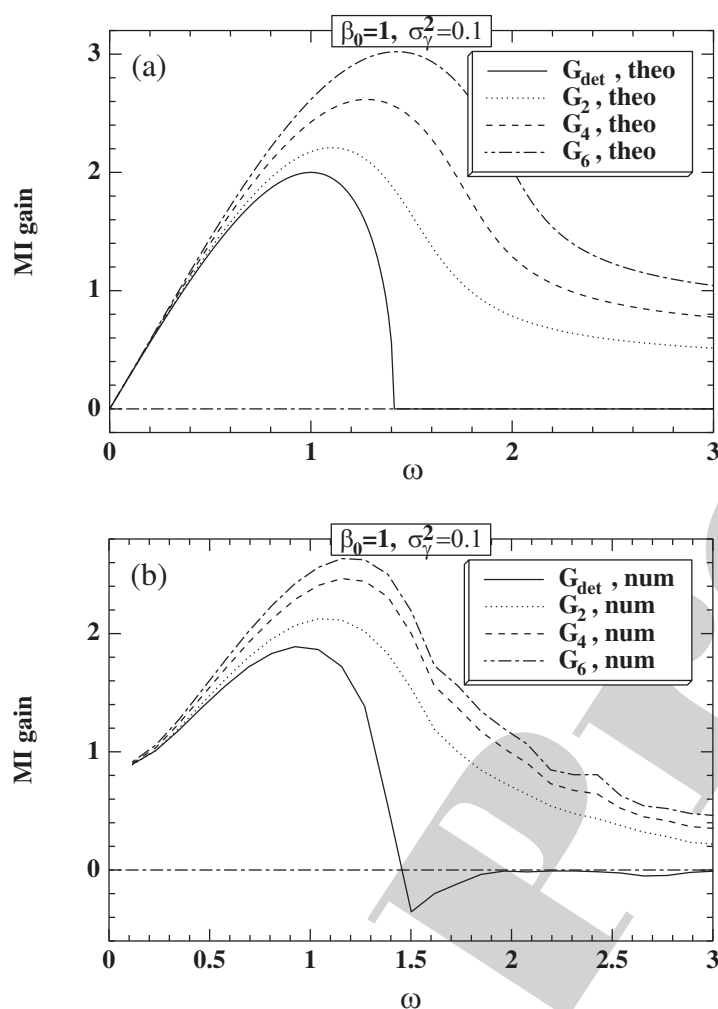


Fig. 3. MI gain curves for $\beta_0 = 1, \gamma_0 P_0 = 1$, deterministic GVD and random nonlinear coefficient with $\sigma_\gamma^2 = 0.1$ ($l = 0.2$ and $\sigma = 1$). The solid curves correspond to the homogeneous case, while the dashed curves correspond to the mean Lyapunov exponents G_{2n} . (a) Theoretical formulas obtained with white-noise approximations. (b) Numerical simulations of stochastic NLSE's averaged over 100 runs.

log-normal distribution has a such heavy tail that the moments of the intensity have very different behaviors. More exactly, the growth of the intensity of the modulation is governed by an expression of the kind $\exp(aW_z + bz)$, where W is a standard Brownian motion. Accordingly, there are different behaviors for the

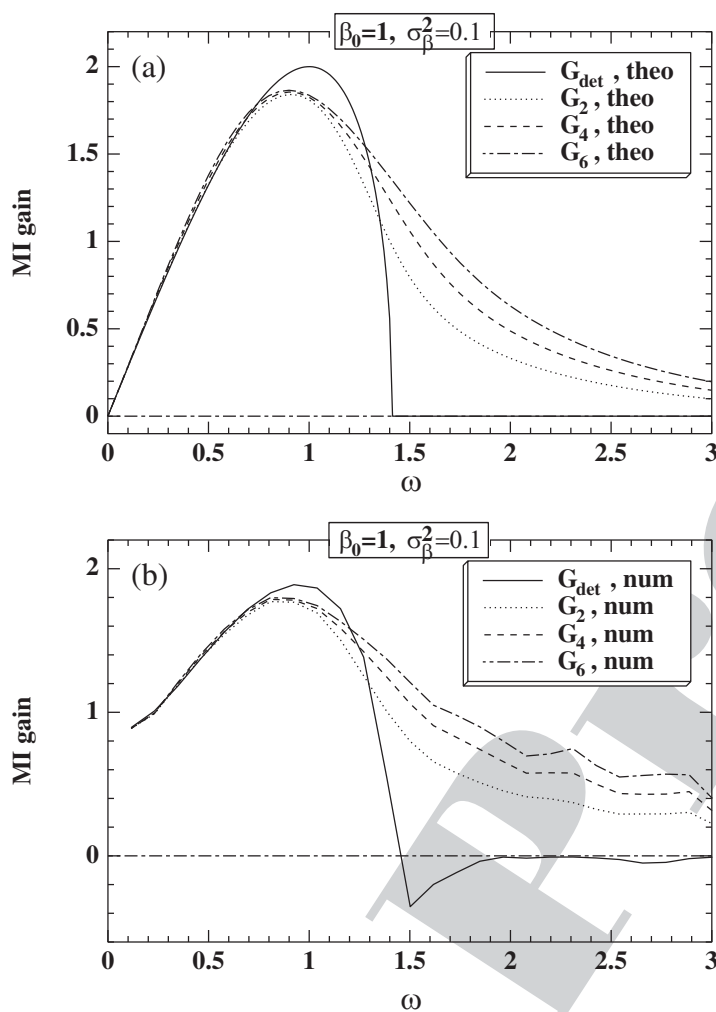


Fig. 4. Same as fig. 3, but now the nonlinear coefficient is homogeneous and the GVD is random, $\sigma_\beta^2 = 0.1$ ($l = 0.2$ and $\sigma = 1$).

mean case and for a typical case, because $W_z \sim \sqrt{z}$ with high probability, but $\langle \exp aW_z \rangle = \exp(\frac{1}{2}a^2z)$. We shall assume for simplicity that the processes m_β and m_γ are independent; the dependent case gives rise to crossed terms that do not qualitatively alter the forthcoming results.

We assume here that either $\beta_0 < 0$ or $\beta_0 > 0$ and that $\beta_0\omega^2 > 2\gamma_0P_0$, i.e. the regions where there is no MI in the homogeneous framework. The sample

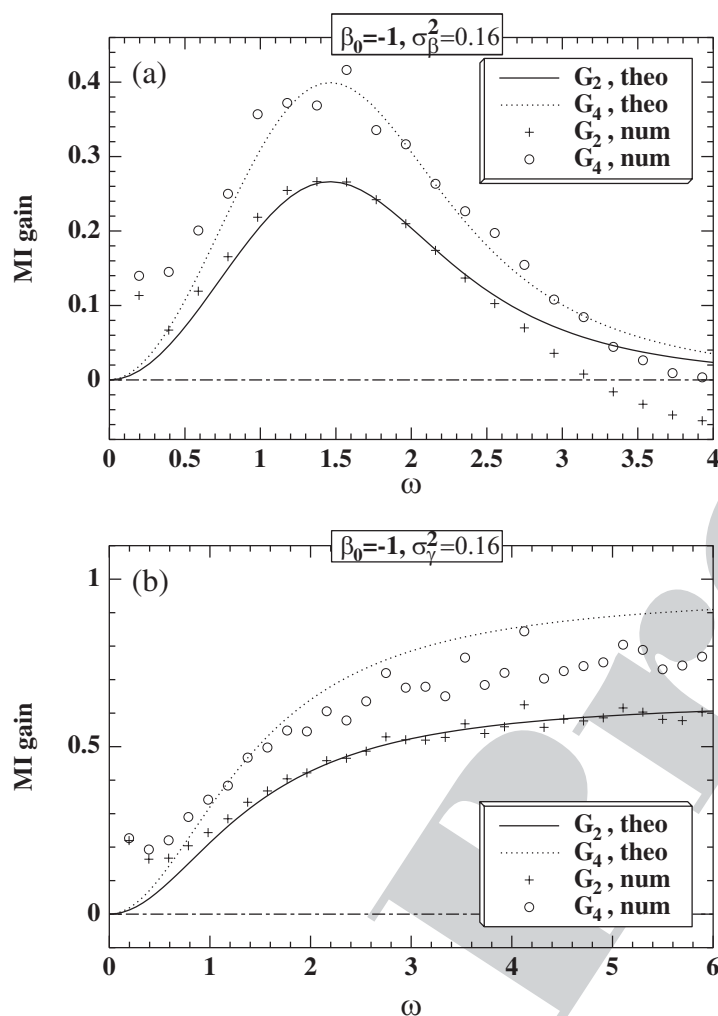


Fig. 5. MI gain spectra for $\beta_0 = -1$, $\gamma_0 P_0 = 1$. (a) Homogeneous nonlinear coefficient and random GVD, with $\sigma_\beta^2 = 0.16$ ($l = 0.02$ and $\sigma = 4$). (b) Homogeneous GVD and random nonlinear coefficient, with $\sigma_\gamma^2 = 0.16$ ($l = 0.02$ and $\sigma = 4$). The curves correspond to the theoretical formulas, while the crosses and circles correspond to the numerical results averaged over 1000 simulations.

and moment Lyapunov exponents have expansions at order 2 with respect to the noise level of the random process:

$$I(z) = I_0 \exp\left(\sqrt{2H(\omega)} W_z + G(\omega)z\right), \quad (4.10)$$

where W_z is a standard Brownian motion, and G is the sample MI gain:

$$G(\omega) = \frac{\beta_0^2 \omega_c^4 \omega^2}{2(\omega_c^2 + \omega^2)} (\alpha_\gamma(\omega) + \alpha_\beta(\omega)), \quad (4.11)$$

with

$$\alpha_j(\omega) = \int_0^\infty \cos\left(2|\beta_0|\omega\sqrt{\omega_c^2 + \omega^2}z\right) \langle m_j(z) m_j(0) \rangle dz, \quad j = \beta, \gamma,$$

and $H(\omega) = G(\omega)$. Note that α_j is non-negative and proportional to the power spectral density of the process m_j by the Wiener–Khinchine theorem (Middleton [1960], p. 141). Accordingly, the $2n$ th-moment MI gain is

$$G_{2n}(\omega) = (n+1)G(\omega).$$

Remember that the sample MI gain is the gain which is actually observed for a typical realization. This provides an affirmative reply to the question whether randomness enhances the MI process in the normal regime.

We now assume that $\beta_0 > 0$ and $\beta_0 \omega^2 < 2\gamma_0 P_0$, i.e. the region where the homogeneous MI gain is positive. The sample and moment Lyapunov exponents have expansions at order 2 with respect to the noise level of the random process (4.10), where the sample MI gain G is

$$G(\omega) = 2\beta_0 \omega \sqrt{\omega_c^2 - \omega^2} - \frac{\beta_0^2 \omega_c^4 \omega^2}{2(\omega_c^2 - \omega^2)} (\bar{\alpha}_\gamma(\omega) + \bar{\alpha}_\beta(\omega)),$$

$$\bar{\alpha}_j(\omega) = \int_0^\infty \exp\left(-2\beta_0 \omega \sqrt{\omega_c^2 - \omega^2}z\right) \langle m_j(z) m_j(0) \rangle dz, \quad j = \beta, \gamma,$$

and H is given by

$$H(\omega) = \frac{\beta_0^2 \omega^2}{\omega_c^2 - \omega^2} \left[(\omega_c^2 - 2\omega^2)^2 \bar{\alpha}_\beta(0) + \omega_c^4 \bar{\alpha}_\gamma(0) \right].$$

Accordingly, the moment MI gains are:

$$G_{2n}(\omega) = G(\omega) + nH(\omega).$$

Analysis of these formulas shows that randomness reduces sample MI peak and optimal frequency:

$$G_{\text{opt}} = \beta_0 \omega_c^2 - \frac{1}{2} \beta_0^2 \omega_c^4 \left(\bar{\alpha}_\gamma(\omega_c/\sqrt{2}) + \bar{\alpha}_\beta(\omega_c/\sqrt{2}) \right),$$

$$\omega_{\text{opt}}^2 = \frac{1}{2} \omega_c^2 - \frac{1}{2} \beta_0 \omega_c^4 \left(\bar{\alpha}_\gamma(\omega_c/\sqrt{2}) + \bar{\alpha}_\beta(\omega_c/\sqrt{2}) \right),$$

but random fluctuations of the nonlinear coefficient involve a highly fluctuating reduction of the MI peak and optimal frequency, so that we actually observe an enhancement of the mean MI peak:

$$G_{2n, \text{opt}} = \beta_0 \omega_c^2 + \beta_0^2 \omega_c^4 \left(n\bar{\alpha}_\gamma(0) - \bar{\alpha}_\gamma \left(\omega_c / \sqrt{2} \right) - \bar{\alpha}_\beta \left(\omega_c / \sqrt{2} \right) \right),$$

$$\omega_{2n, \text{opt}}^2 = \frac{1}{2} \omega_c^2 + \frac{1}{2} \beta_0 \omega_c^4 \left(n\bar{\alpha}_\gamma(0) - \bar{\alpha}_\gamma \left(\omega_c / \sqrt{2} \right) - \bar{\alpha}_\beta \left(\omega_c / \sqrt{2} \right) \right),$$

while random fluctuations of GVD involve a deterministic reduction of the MI peak and optimal frequency. These surprising effects can also be observed in figs. 3b and 4b.

4.2.6. Conclusions

Stochastic parametric resonances between the wavevectors of the perturbations and those of the modes of the linearized systems lead to MI for normal dispersion. The results represent a straightforward generalization of those obtained in the previous section for periodic variations of the fiber parameters. Because a random variation contains all frequencies, the parametric resonance arises for any frequency of the modulation.

For anomalous dispersion the domain of MI increases, accompanied by a reduction of MI gain. More precisely the MI gain peak for almost every realization is described by a non-random quantity in case of GVD fluctuations, where only the Laplace transform of the autocorrelation function of the random process at the optimal frequency appears. In case of fluctuations of the nonlinear coefficient, the results show that the MI peak is reduced in probability, but is enhanced in mean, because there exist some rare events (i.e. realizations of the fluctuations of the nonlinear coefficient) for which the MI peak is drastically increased, and these rare events impose the mean value.

4.3. MI in fibers with random birefringence

We have seen that scalar MI in homogeneous media only occurs when the GVD is negative (anomalous regime). Cross-phase modulation (XPM) between two modes may extend the instability domain to the normal dispersion regime (Agrawal [1987]). This XPM-induced MI is also called Vector Modulational Instability (VMI).

4.3.1. VMI induced by random nonlinearity and GVD

The MI of nonlinear continuous waves in birefringent fibers with random dispersion has been analyzed by Abdullaev and Garnier [1999]. The effects of random fluctuations of the chromatic dispersion are very similar to the scalar case. More exactly it is found that in the normal dispersion region all frequencies are modulationally unstable. In the anomalous case the MI spectrum is broadened and the MI gain is reduced. Although analyses have never been performed, the conjecture is that random fluctuations of the nonlinear coefficient give rise to effects that are similar to those observed in the scalar case. The analysis of vector MI induced by random birefringence is more interesting in that birefringence is the fiber parameter that exhibits the most important fluctuations, and it gives rise to the most interesting effects.

4.3.2. VMI induced by random birefringence and PMD

The evolution of polarized fields in randomly birefringent fibers is governed by the coupled NLS equations (Wai and Menyuk [1996]):

$$i\vec{A}_z + \mathbf{K}\vec{A} + i\mathbf{\Delta}\vec{A}_t + \beta\vec{A}_{tt} + \frac{\gamma}{8}\vec{N}_1 = 0, \quad (4.12)$$

where \vec{A} is the column vector $(A_1, A_2)^T$ that denotes the envelopes of the electric field in the two eigenmodes (polarizations); we use standard dimensionless variables. The matrices \mathbf{K} and $\mathbf{\Delta}$ describe random fiber birefringence. The GVD coefficient is β . The \vec{N}_1 term stands for the nonlinear terms:

$$\vec{N}_1 = \begin{pmatrix} (|A_1|^2 + \alpha|A_2|^2)A_1 + \frac{\alpha}{2}A_2^2A_1^* \\ (|A_2|^2 + \alpha|A_1|^2)A_2 + \frac{\alpha}{2}A_1^2A_2^* \end{pmatrix}, \quad (4.13)$$

where the cross-phase modulation is $\alpha = \frac{2}{3}$ for linearly birefringent fiber.

As shown by Wai and Menyuk [1996], one can eliminate the fast random birefringence variations that appear in eq. (4.12) by means of a change of variables leading to the new vector equation

$$i\vec{U}_z + i\mathbf{\Omega}\vec{U}_t + \beta\vec{U}_{tt} + \gamma\vec{N}_2 = 0, \quad (4.14)$$

where $\vec{U} \equiv \mathbf{M}^{-1}\vec{A}$ and $\vec{U} = (u, v)^T$ represents the slow evolution of the field envelopes in the reference frame of the local polarization eigenmodes, and the matrix \mathbf{M} obeys the equation $i\mathbf{M}_z + \mathbf{K}\mathbf{M} = 0$. The nonlinear term \vec{N}_2 reads

$$\vec{N}_2 = \begin{pmatrix} (|u|^2 + \alpha|v|^2)u \\ (\alpha|u|^2 + |v|^2)v \end{pmatrix}, \quad (4.15)$$

where the cross-phase modulation $\alpha = 1$ after averaging over fiber birefringence (Evangelides, Mollenauer, Gordon and Bergano [1992]). $\mathbf{\Omega}$ is a z -dependent matrix associated with the coupling between the modes due to perturbations:

$$\mathbf{\Omega}(z) = \begin{pmatrix} 0 & 1 \\ 1 & 0 \end{pmatrix} S_1(z) + \begin{pmatrix} 0 & -i \\ i & 0 \end{pmatrix} S_2(z) + \begin{pmatrix} 1 & 0 \\ 0 & -1 \end{pmatrix} S_3(z), \quad (4.16)$$

where S_j are white Gaussian-distributed noises:

$$\langle S_j(z) \rangle = 0, \quad \langle S_j(z) S_j(z') \rangle = 2\sigma^2 \delta(z - z'), \quad j = 1, 2, 3.$$

The presence of the term $\mathbf{\Omega} \vec{U}_t$ is associated with linear coupling between the modes, as well as an accumulation of a mismatch between their phases. In spite of this extension the model remains analytically solvable and it predicts general new features associated with the random nature of polarization MI.

The nonlinear continuous-wave solutions of the system (4.14) read as $u_0(z) = A \exp(i\gamma(A^2 + B^2)z)$ and $v_0(z) = B \exp(i\gamma(A^2 + B^2)z)$. Linear stability is evaluated by substituting

$$u(z, t) = (A + u_1(z, t)) \exp[i\gamma(A^2 + B^2)z],$$

$$v(z, t) = (B + v_1(z, t)) \exp[i\gamma(B^2 + A^2)z],$$

into eq. (4.14). By retaining only the first-order terms one obtains a linear system of equations for u_1 and v_1 :

$$iu_{1z} + iS_1 v_{1t} + S_2 v_{1t} + iS_3 u_{1t} + \beta u_{1tt} + 2\gamma [A^2 \operatorname{Re}(u_1) + AB \operatorname{Re}(v_1)] = 0,$$

$$iv_{1z} + iS_1 u_{1t} - S_2 u_{1t} - iS_3 v_{1t} + \beta v_{1tt} + 2\gamma [B^2 \operatorname{Re}(v_1) + AB \operatorname{Re}(u_1)] = 0.$$

The MI gains are defined as the Lyapunov exponents that govern the exponential growths of the Fourier components of the modulations u_1 and v_1 .

In the anomalous dispersion regime it has been found by Garnier, Abdullaev, Seve and Wabnitz [2001] that the MI region is increased by random birefringence so that all frequencies are unstable as soon as $\sigma^2 > 0$ while the MI peak is reduced. Denoting by $P_0 = A^2 + B^2$ the total power, the MI peak is equal to $2\gamma P_0$ when $\sigma = 0$, and it decays as σ increases. The first terms of the asymptotic

expansion of the MI gain in the limit of small noise $\beta^{-1}\sigma^2 \ll 1$ can be computed. For $\omega < \omega_c := \sqrt{2\gamma P_0/\beta}$, the MI gain is reduced:

$$G_2(\omega) = 2\beta\omega\sqrt{\omega_c^2 - \omega^2 - 4\omega^2\sigma^2}. \quad (4.17)$$

The MI peak $G_{2,\text{opt}} = \beta\omega_c^2 - 2\sigma^2\omega_c^2$ is obtained at $\omega_{2,\text{opt}}^2 = \frac{1}{2}\omega_c^2 - \sigma^2\omega_c^2/\beta$. For $\omega > \omega_c$ the MI gain is positive, while it is zero for $\sigma = 0$:

$$G_2(\omega) = 4\omega^2 \frac{2K_0K_1(\omega) - 2K_0^2(\omega) + 5\gamma^2 P_0^2 \beta^{-2}}{3K_0K_1(\omega) + 5K_0^2(\omega) - 5\gamma^2 P_0^2 \beta^{-2}} \sigma^2, \quad (4.18)$$

where $K_0(\omega) = \omega^2 - \gamma P_0 \beta^{-1}$, $K_1(\omega) = \omega\sqrt{\omega^2 - 2\gamma P_0 \beta^{-1}}$.

In the normal dispersion regime all frequencies are made unstable by random birefringence. As in the case $\beta > 0$, the closed-form expression for the MI gain is too complicated to be written down explicitly. Nevertheless the first terms of the asymptotic expansion of the MI gain for small PMD fluctuations $|\beta|^{-1}\sigma^2 \ll 1$ can be computed. It is found that for any $\omega > 0$ the MI gain is positive and given by (4.18). The MI gain spectrum is maximal for $\omega_{2,\text{opt}} = (\sqrt{2} - 1)^{1/2} \sqrt{\gamma P_0 / |\beta|}$ and the corresponding MI peak is

$$G_{2,\text{opt}} = \frac{2(\sqrt{2} - 1)(2\sqrt{2} + 1)}{5 + 3\sqrt{2}} \frac{\gamma P_0 \sigma^2}{|\beta|}.$$

4.4. The case of a random-in-time potential

We shall now say few words about the case of a potential that is random in time. The model is the nonlinear Schrödinger equation:

$$iu_z + \beta u_{tt} + \gamma |u|^2 u = V(t) u, \quad (4.19)$$

where $V(t)$ is a random time-dependent potential. We could also consider temporal fluctuations of the nonlinear coefficient $\gamma(t)$ or the GVD coefficient $\beta(t)$. First of all we would like to point out that the problem at hand is different from the homogeneous or spatially random problems in that there is no continuous-wave solution of eq. (4.19). Therefore the question of the stability of such a stationary wave is meaningless. Actually it is well-known that in linear and random media all eigenstates of the Schrödinger operator are localized (Anderson [1958]). Previous work on the stationary NLS equation has shown strong evidence that there exist delocalized transmission states (Doucot and Rammal [1987]). However,

since only the time-harmonic problem has been addressed, not all of these states are physical, so that a complete study with the time-dependent model (4.19) is required to understand this issue. Numerical experiments have been performed by Caputo, Newell and Shelley [1990]. An input pulse that decomposes into lumps without randomness (standard MI) has been shown to generate new pulses that are NLS solitons. Indeed, solitons are normal propagating modes for the homogeneous NLS equation. A lot of work was then devoted to the propagation of solitons across random media. Theoretical (Kivshar, Gredeskul, Sánchez and Vázquez [1990]) and numerical studies (Knapp [1995]) have demonstrated that, for a NLS soliton propagating in a random medium, there exist two distinct regimes of behavior which depend on the soliton parameters. One of these regimes has been shown to be very different from the localization regime in that the soliton retains its mass although it loses velocity.

§ 5. MI in nonlinear discrete optical systems

To date, quickly developing technologies like epitaxial growth, ion exchange in solids, electrical poling, etc., permit the fabrication of new kinds of thin films, multilayered systems, and different photonic band-gap structures for advanced photonics applications. The discrete nature of such structures gives rise to qualitatively new types of excitations and effects connected with them. Arrays of coupled waveguides represent a prominent example of discrete optical systems, where interplay between inherent discreteness and nonlinearity qualitatively alter the dynamical behavior compared with their continuous counterparts. In particular, spreading of the initial excitation due to linear coupling, which can be viewed as effective discrete diffraction, can be compensated by nonlinearity-induced localization. As a result, localized modes, frequently referred to as discrete solitons (DSs) are formed. Since the original investigations (Dolgov [1986], Sievers and Takeno [1988], Page [1990]) a considerable and steadily growing amount of interest has focused on the study of these localized modes in nonlinear discrete systems because of their relevance in various fields such as solid-state physics, optics, and biology (Scott [1992], Flach and Willis [1998], Hennig and Tsironis [1999], Lederer, Darmanyan and Kobayakov [2001]). Different kinds of bright and dark DSs may exist in this environment (Cristodoulides and Joseph [1988], Cai, Bishop and Grønbech-Jensen [1994], Konotop and Salerno [1997], Darmanyan, Kobayakov and Lederer [1998b], Hennig and Tsironis [1999]), where MI of the nonlinear plane-wave solution is a necessary condition for bright soliton formation. Dark DSs, on the

contrary, need a modulationally stable background. Experimental demonstrations of these phenomena in nonlinear mechanical and electrical lattices have been reported by Denardo, Galvin, Greenfield, Larraza, Putterman and Wright [1992] and Marquie, Bilbaut and Remoissenet [1995]. Specific features of the MI and recurrence phenomena as well as pattern formation in nonlinear lattices have been discussed by Kivshar and Peyrard [1992], Kivshar, Haelterman and Sheppard [1994], Burlakov, Darmanyan and Pyrkov [1995], Burlakov, Darmanyan and Pyrkov [1996], Daumont, Dauxois and Peyrard [1997], Leon and Manna [1999], Burlakov [1998] and Vanossi, Rasmussen, Bishop, Malomed and Bortolani [2000]. In particular, it has turned out that a peculiar feature of many discrete systems consists in the critical dependence of both the MI gain and the MI domain on the wavenumber related to the discrete variable. Nonlinear optical waveguide arrays have been proposed as the basis for different schemes of all-optical signal processing and switching (Bang and Miller [1996], Krolikowski and Kivshar [1996], Aceves, De Angelis, Peschel, Muschall, Lederer, Trillo and Wabnitz [1996], Peschel, Muschall and Lederer [1997], Darmanyan, Kobayakov and Lederer [1998b]). Experimental observations of ultrafast switching as well as existence and dynamics of DSs were reported for arrays fabricated on the basis of AlGaAs (Millar, Aitchison, Kang, Stegeman, Villeneuve, Kennedy and Sibbett [1997], Eisenberg, Silberberg, Morandotti, Boyd and Aitchison [1998], Morandotti, Peschel, Aitchison, Eisenberg and Silberberg [1999]). As mentioned above, the stability of nonlinear solutions is an important property which drastically affects the entire dynamics. This is of particular importance for a nonintegrable discrete system where many solutions can be found only approximately. In the following we consider stability of discrete plane-wave solitons in an array of n lossless, identical and equidistant channel waveguides or fibers. The dynamics of this system, as well as of many others, is described by the discrete nonlinear Schrödinger equation (DNLSE) or by its modifications depending on the kind of nonlinearity, the scalar or vector nature of the system, etc. In § 5.1 we will be dealing with the MI of discrete plane-wave solitons of scalar and vectorial DNLSE with Kerr-like nonlinearity; we consider the case of quadratic nonlinearity in § 5.2. Finally, § 5.3 is devoted to the study of the influence of temporal effects on the MI in an array with cubic nonlinearity.

5.1. MI in discrete cubic media

For generality we start with the vectorial case where two components with different frequencies or polarization states copropagate in a nonlinear waveguide.

In this case the cubic nonlinearity provides a self-phase modulation (SPM) of each field component as well as a nonlinear coupling between the components resulting in cross-phase modulation (XPM) and energy exchange. The latter effect can be neglected provided that the wavevector mismatch between both field components is large. In continuous systems the field dynamics can then be described by two incoherently coupled NLSEs, the properties and solutions of which have been studied extensively. In turn, in the discrete case the two-component field dynamics is described by two coupled DNLSs constituting the following set of difference-differential equations:

$$i \frac{dA_n}{dZ} + C_1(A_{n-1} + A_{n+1}) + (\lambda_{11}|A_n|^2 + \lambda_{12}|B_n|^2)A_n = 0, \quad (5.1)$$

$$i \frac{dB_n}{dZ} + C_2(B_{n-1} + B_{n+1}) + (\lambda_{21}|A_n|^2 + \lambda_{22}|B_n|^2)B_n = 0, \quad (5.2)$$

where A_n and B_n represent the field envelopes of both components in the n th channel, the evolution variable Z denotes the spatial coordinate along the waveguide, and $C_{1,2} = \pi/2L_{1,2}$ are the respective coupling coefficients, with $L_{1,2}$ the half beat lengths of the corresponding two-core coupler. The effective nonlinear coefficients $\lambda_{i,j} = \omega_i n_{i,j} \sigma_{i,j} / 2c$ ($i, j = 1, 2$) with $\sigma_{i,j} = \int dx dy |R_i|^2 |R_j|^2 / \int dx dy |R_i|^4$ include the dimensionless functions $R_i(x, y)$ describing the transverse mode profile and the cubic nonlinear coefficients n_{ij} . For weakly guided modes in optical fibers we have $\sigma_{i,j} \approx 0.5$ (Agrawal [1995], Abdullaev, Darmanyan and Khabibullaev [1993]). The existence and stability of bright and dark vectorial discrete solitons as well as MI of plane waves in the system described by eqs. (5.1) has been studied by Kobayakov, Darmanyan, Lederer and Schmidt [1998] and Darmanyan, Kobayakov, Schmidt and Lederer [1998].

Equations (5.1) can be recast in a more convenient dimensionless form:

$$i \frac{da_n}{dz} + c_a(a_{n-1} + a_{n+1}) + (\lambda_a|a_n|^2 + |b_n|^2)a_n = 0, \quad (5.3)$$

$$i \frac{db_n}{dz} + c_b(b_{n-1} + b_{n+1}) + (|a_n|^2 + \lambda_b|b_n|^2)b_n = 0,$$

where $a_n = |\lambda_{21}/\lambda_{12}|^{1/2} A_n/B_{\max}$, $b_n = B_n/B_{\max}$, $z = Z/L_{\text{NL}}$, $L_{\text{NL}}^{-1} = \lambda_{12}|B_{\max}|^2$, $c_{a,b} = C_{1,2}L_{\text{NL}}$, $\lambda_a = \lambda_{11}/\lambda_{12} > 0$, $\lambda_b = \lambda_{22}/\lambda_{12} > 0$, and B_{\max} is the peak amplitude of the second field component.

Provided that the field envelopes vary slowly with n , eqs. (5.3) can be transformed into a continuous system which describes likewise pulse propagation

in a dispersive medium and beam evolution in a planar waveguide with SPM and XPM. For the specific case of equal SPM and XPM coefficients the corresponding continuous system has been proven to be integrable. A discussion of various peculiarities of the continuous system, including the formation of bright and dark solitons as well as modulational instability of plane wave solutions, can be found for arbitrary ratios between SPM and XPM coefficients in the article by Agrawal [1995].

As in the continuous model the system (5.3) describes coupling between modes which either oscillate at different frequencies ($\lambda_a \approx \lambda_b \approx 0.5$) or are orthogonally polarized in a highly birefringent waveguide. In the case of an elliptically birefringent fiber $\lambda_a = \lambda_b = \lambda$, where λ varies between 0.5 and 1.5 depending on the angle of ellipticity. Let us consider the MI of the stationary plane-wave solution to eqs. (5.3) that has the form

$$a_n = a \exp [i (q_a n + k_a z)], \quad b_n = b \exp [i (q_b n + k_b z)], \quad (5.4)$$

where

$$k_a = 2c_a \cos q_a + \lambda_a a^2 + b^2, \quad k_b = 2c_b \cos q_b + \lambda_b b^2 + a^2. \quad (5.5)$$

To investigate the stability of this solution we substitute into eqs. (5.3) a slightly perturbed eq. (5.4), namely, $\bar{a}_n = (a + \xi_n(z)) \exp [i (q_a n + k_a z)]$, $\bar{b}_n = (b + \zeta_n(z)) \exp [i (q_b n + k_b z)]$, where

$$\begin{aligned} \xi_n(z) &= u_1 \exp [i (Qn + Kz)] + u_2 \exp [-i (Qn + K^*z)], \\ \zeta_n(z) &= v_1 \exp [i (Qn + Kz)] + v_2 \exp [-i (Qn + K^*z)]. \end{aligned} \quad (5.6)$$

Performing linearization with respect to small perturbation we end up with the following eigenvalue problem for the perturbation wave vector K :

$$\det \begin{bmatrix} -K + f_+ & \lambda_a a^2 & a^2 b^2 & a^2 b^2 \\ \lambda_a a^2 & K + f_- & a^2 b^2 & a^2 b^2 \\ a^2 b^2 & a^2 b^2 & K + g_+ & \lambda_b b^2 \\ a^2 b^2 & a^2 b^2 & \lambda_b b^2 & -K + g_- \end{bmatrix} = 0, \quad (5.7)$$

where $f_{\pm} = 2c_a [\cos(q_a \pm Q) - \cos q_a] + \lambda_a a^2$, $g_{\pm} = 2c_b [\cos(q_b \pm Q) - \cos q_b] + \lambda_b b^2$. Thus, according to eq. (5.6), $G = |\text{Im}K|$ provides us with the MI gain. To resolve the eigenvalue problem (5.7) one needs to apply numerical methods. However in some particular cases it can be treated analytically. In what follows

we consider two of these cases important for applications, viz., (i) scalar DNLSE and (ii) vectorial DNLSE at $q = 0, \pi$.

5.1.1. Scalar DNLSE

For the scalar DNLSE ,

$$i \frac{db_n}{dz} + c(b_{n-1} + b_{n+1}) + \lambda |b_n|^2 b_n = 0, \quad (5.8)$$

i.e. for $a = c_a = \lambda_a = 0$, the eigenvalue problem (5.7) reduces to that considered by Kivshar and Peyrard [1992]. The solution in this case can be found easily:

$$K = -2c \sin Q \sin q \pm \sqrt{8c \sin^2(\frac{1}{2}Q)(2c \cos^2 q \sin^2(\frac{1}{2}Q) - \lambda b^2 \cos q)}. \quad (5.9)$$

Thus for $\lambda \cos q > 0$ the plane-wave solution of the scalar DNLSE is modulationally unstable with the gain

$$G = 2 \left| \sin(\frac{1}{2}Q) \right| \sqrt{2c \cos q (\lambda b^2 - 2c \cos q \sin^2(Q/2))}. \quad (5.10)$$

It is important to note that for $\cos q < 0$, MI occurs in defocusing media where $\lambda < 0$. This is in contrast with MI in the continuous case, which can be reproduced from eq. (5.10) by inserting $\cos q = 1$, $\sin Q \approx Q$.

5.1.2. Vector DNLSE at $q = 0, \pi$

It can be inferred from eqs. (5.7) and (5.10) that the stability of the plane-wave solution (5.4) strongly depends on the carrier wavevectors. This, as mentioned above, is an intrinsic feature of discrete systems which distinguishes them from the continuous analogues. We note that for the strongly localized soliton-like solutions, amplitudes in two adjacent channels are either in phase (so-called unstaggered solution $q = 0$) or out of phase (staggered solution $q = \pi$). In what follows, for simplicity, we restrict ourselves to these two cases. This allows a simplification of eq. (5.7), i.e. for $q = 0, \pi$ it can be reduced to the biquadratic equation

$$K^4 + p_1 K^2 + p_0 = 0 \quad (5.11)$$

with the coefficients

$$p_0 = f^2 g^2 - \lambda^2 [a^4 g^2 + b^4 f^2 + a^4 b^4 (4 - \lambda^2)] + 2a^2 b^2 (\lambda g a^2 + \lambda f b^2 - fg), \quad (5.12)$$

$$p_1 = \lambda^2 (a^4 + b^4) - f^2 - g^2, \quad (5.13)$$

$$f = \lambda a^2 - 2c_a (1 - \cos Q), \quad g = \lambda b^2 - 2c_b (1 - \cos Q). \quad (5.14)$$

Here we have assumed $\lambda_a = \lambda_b = \lambda$ (different polarizations) and $\text{sgn}(c_{a,b}) = \text{sgn}(\lambda_{ij} \cos q_{a,b})$. Thus, provided that $C_{1,2} > 0$, which is the only case that is

physically meaningful, and $\lambda_{ij} > 0$ (focusing nonlinearity) hold, the normalized linear coupling $c_{a,b}$ is positive (negative) for $q_{a,b} = 0$ (π), respectively. Note that the vector DNLSE can support solutions where an unstaggered component is coupled with a staggered one (e.g. $q_a = 0$, $q_b = \pi$), viz. $c_a = -c_b$.

The MI gain can be calculated straightforwardly from eq. (5.11) as

$$G = \left| \operatorname{Im} \sqrt{\frac{1}{2} \left(-p_1 \pm \sqrt{p_1^2 - 4p_0} \right)} \right|. \quad (5.15)$$

It equals zero if $0 < p_0 < \frac{1}{4}p_1^2$ and $p_1 < 0$ hold. For equal moduli of the coupling coefficients, $|c_a| = |c_b|$, eq. (5.11) exhibits zero gain for $0 < Q < \pi$ only provided that

$$c_a = c_b < 0, \quad \lambda \geq 1, \quad (5.16)$$

or

$$c_a = -c_b > 0, \quad 2a/(a^2 + 1) \leq \lambda \leq 1, \quad (5.17)$$

where without loss of generality we assumed $a < b = 1$. The solution (5.4) is modulationally unstable in those regions of parameter space where eqs. (5.16) and (5.17) are not satisfied.

The respective gain is plotted in fig. 6 as a function of the amplitude of the first component a and the nonlinearity λ . As predicted by eqs. (5.15) and (5.16), the vectorial unstaggered ($q_{a,b} = 0$) plane-wave solution is always unstable in a medium with focusing nonlinearity ($\lambda_{ij} > 0$) (see fig. 6a), which coincides with the behavior of the corresponding scalar mode. However, if both components are staggered the mode is stable only for $\lambda \geq 1$ (see eq. 5.16 and fig. 6b). A vectorial solution which consists of one unstaggered and one staggered wave can be stable only if the weaker component is unstaggered (unstable in the scalar limit) and, in addition, eq. (5.17) is satisfied (see fig. 6c). This condition defines a boundary between the stable and unstable regions: a small periodic perturbation corresponding, e.g., to point S ($\lambda = 0.8$) in fig. 6c does not grow and the plane wave propagation is stable. However, if the amplitude of the A -component is slightly increased and exceeds a critical value (point T in fig. 6c), the same small perturbation (1% of the wave amplitude) leads to the formation of a nonstationary cnoidal-like wave (fig. 7).

If the stronger component is unstable in the scalar limit, i.e. $c_a = -c_b < 0$, this vectorial solution is always unstable (fig. 6d). The nonmonotonic behavior of the

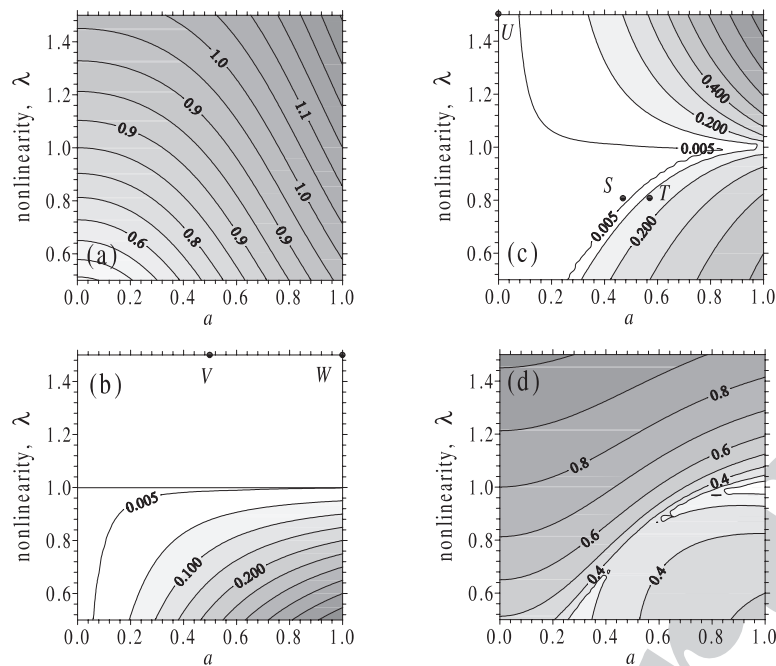


Fig. 6. Maximum MI gain as a function of the amplitude of the first component $a(b = 1)$ and the nonlinear coupling λ ; (a) $c_a = c_b = 0.1$, (b) $c_a = c_b = -0.1$, (c) $c_a = -c_b = 0.1$, (d) $-c_a = c_b = 0.1$.

gain in fig. 6d arises from the fact that the maximum gain is shifted from the edge of the Brillouin zone, $Q = \pi$, to its center. This shift can also be recognized in fig. 8, where the maximum gain is plotted as a function of linear coupling (equal for both components) together with the respective value of Q . For larger $c_{a,b}$ the maximum gain tends to saturate and the respective value of Q decreases. Thus, no qualitative difference in stability behavior arises upon a change in the linear coupling.

The existence of stable regions (see figs. 6b,c) is a prerequisite for the formation of vector dark solitons. An interesting feature of the system studied here consists in the instability of the vectorial plane-wave solution for a certain strength of the nonlinear coupling where either component is stable in the scalar limit. The analysis has shown that the case of equal self- and cross-phase modulation coefficients represents an interesting situation in the discrete scenario as well. As a matter of fact, it represents a stability boundary for solutions consisting of a staggered and an unstaggered component.

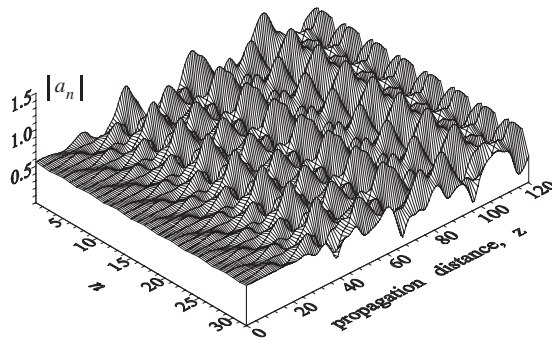


Fig. 7. Modulational instability of the periodically perturbed plane wave solution corresponding to point T in fig. 6c; the a -component is shown, the b -component has a similar structure. The waveguides are labelled by positive numbers. Parameters: $c_a = -c_b = 0.1$, $\lambda_a = \lambda_b = 0.8$, $a = 0.55$, $b = 1$, $Q = \frac{1}{2}\pi$.

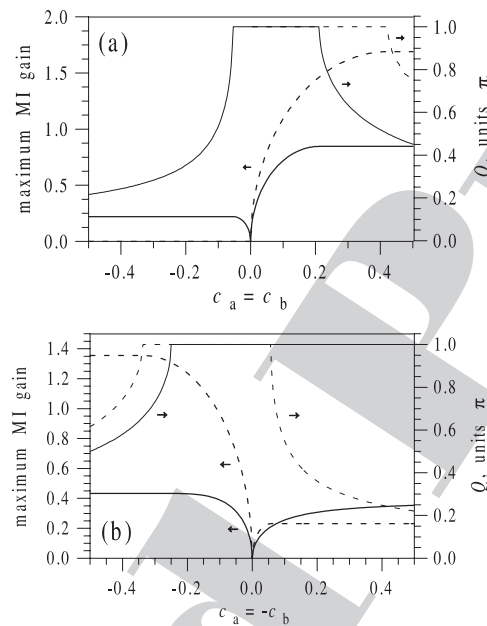


Fig. 8. Maximum instability gain and the respective wavevector of modulation Q as a function of linear coupling for the two components; (a) $c_a = c_b$, (b) $c_a = -c_b$. Parameters: $a = 0.5$, $b = 1$; solid curves $\lambda_a = \lambda_b = 0.5$, dashed curves $\lambda_a = \lambda_b = 1.5$.

5.2. MI in discrete quadratic media

It is a common belief that, compared to the cubic scenario, a quadratic nonlinearity provides a greater variety of effects and, more importantly, that they are obtainable for lower optical power. The particular form of the nonlinearity leads to energy exchange between the field components and additionally brings another crucial parameter, the phase mismatch, into play. Although the equations describing the field dynamics in such media are not integrable, stable mutually locked solitary waves may exist, as was experimentally confirmed in continuous bulk media (Torruelas, Wang, Hagan, Van Stryland, Stegeman, Torner and Menyuk [1995]) and in film waveguides (Schiek, Baek and Stegeman [1996]). As far as discrete media with quadratic nonlinearity is concerned the existence of different families of bright and dark localized two-field states has been demonstrated theoretically, and their fundamental properties have been studied (Peschel, Peschel and Lederer [1998], Darmanyan, Kobayakov and Lederer [1998a], Miller and Bang [1998], Kobayakov, Darmanyan, Pertsch and Lederer [1999]). In this subsection we consider the MI of a two-component plane wave in such an environment.

The evolution of the two-component field in a waveguide array with quadratic nonlinearity may be described by the following proper normalized set of difference-differential equations (Kobayakov, Darmanyan, Pertsch and Lederer [1999]):

$$\begin{aligned} i \frac{da_n}{dz} + c_a(a_{n-1} + a_{n+1}) + 2\gamma a_n^* b_n &= 0, \\ i \frac{db_n}{dz} + c_b(b_{n-1} + b_{n+1}) + \beta b_n + \gamma a_n^2 &= 0, \end{aligned} \quad (5.18)$$

where z denotes the propagation direction, a_n and b_n are the amplitudes of the fundamental (FW) and second-harmonic (SH) guided waves, $c_{a,b}$ and γ are linear and quadratic nonlinear coupling coefficients, respectively, and β is the wavevector mismatch. Equations (5.18) remind of the well-known system describing the evolution of spatial solitons in a quadratically nonlinear film waveguide where diffraction is replaced by linear coupling. It is evident that in the long-wavelength case (slow variation with n) the dynamic equations (5.18) transform into the continuum limit. As mentioned above, several types of localized solutions to this system have been found both in continuous and in discrete cases, while the discrete case provides more variety of DS solutions.

To find the stationary plane-wave solutions to the set (5.18) we insert the ansatz

$$a_n = a \exp [i(qn - kz)], \quad b_n = b \exp [2i(qn - kz)]. \quad (5.19)$$

This gives us a relation between the FW and SH amplitudes a and b as

$$a^2 = 4b^2 + \frac{b(4c_a \cos q - 2c_b \cos 2q - \beta)}{\gamma} > 0, \quad (5.20)$$

and the dispersion law which relates the wavevector in the propagation direction (k) with the transverse wavevector (q) and the SH amplitude b :

$$k = -2(c_a \cos q + \gamma b). \quad (5.21)$$

As a matter of fact, a certain SH amplitude b applies to a FW amplitude a of either sign.

To check the stationary plane-wave solution (5.19)–(5.21) against MI we repeat all steps of the linear stability analysis of two-component fields described above for the array with cubic nonlinearity. Considering, for the same reason as in the previous subsection, the cases of $q = 0, \pi$ we arrive at the conclusion that MI gain G is described by eq. (5.15) where, instead of eqs. (5.12)–(5.14), parameters p_0 and p_1 are given by the following expressions:

$$p_0 = f^2 g^2 + 16\gamma^4 a^4 - 4\gamma^2 b^2 g^2 - 8\gamma^2 a^2 f g, \quad (5.22)$$

$$p_1 = 4\gamma^2 (b^2 - 2a^2) - f^2 - g^2, \quad (5.23)$$

$$f = 2\gamma b \pm 2c_a(1 - \cos Q), \quad g = 4\gamma b \pm 4c_a - 2c_b \cos Q - \beta, \quad (5.24)$$

where the upper (lower) sign applies to $q = 0$ ($q = \pi$).

In the long-wavelength limit (small Q) the MI gain approaches that of the continuum model (Trillo and Ferro [1995]). The maximum MI gain is plotted in fig. 9 as a function of the stationary SH amplitude b and the mismatch β for in-phase ($q = 0$) and out-of-phase ($q = \pi$) solutions. With regard to the dispersion relation (5.21) these two cases correspond to opposite signs of dispersion of the linear waves. Evidently the change of the character of dispersion critically affects the stability behavior. Although the stability ranges for the two regimes differ considerably, a common stable region with ($b < 0$ and $\beta < 0$) can be identified. To illustrate the effect of the MI of the plane-wave solution it is appropriate to consider evolution of dark solitons.

The consequences of the background stability for the dynamics of dark DSs is shown in fig. 10, where the propagation of two dark kink-like DSs which are in close proximity in the b – β plane is displayed. The obviously stable DS corresponds to the domain where $G = 0$ holds (fig. 10a). A slight change of the SH amplitude b causes the solution to move to the unstable region. As a result the dark DS gets unstable and decays after some distance (fig. 10b).

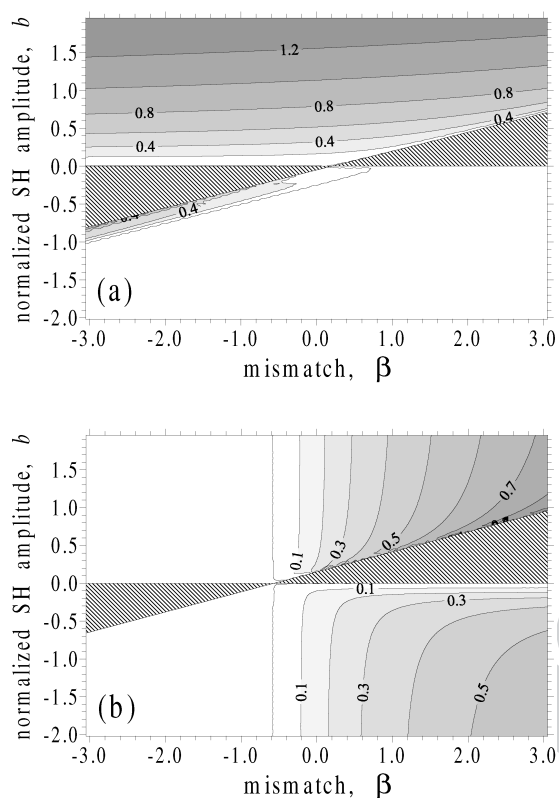


Fig. 9. Maximum MI gain as a function of the normalized SH amplitude and the wavevector mismatch. No plane-wave solution exists in the shaded region. Bright regions correspond to stable solutions ($G = 0$). Parameters: $c_a = c_b = 0.1$; (a) $q = 0$, (b) $q = \pi$.

5.3. Temporal effects in arrays with cubic nonlinearity

To study the propagation of short pulses in waveguide arrays one needs to take into account the dispersion that acts in each channel of the array. In this case an additional variable, time, appears in the governing equation. The equation becomes 1+2 type, where along with the evolution variable there are two others, one of which is discrete and the second is continuous. Such a discrete–continuous combination introduces new interesting features into the system dynamics. In particular, the discreteness stops the collapse that takes place in fully continuous 1+2 systems, and leads to the formation of stable 2D-localized structures. The existence and stability of solitary waves localized both along (temporally) and across the array have been considered by Aceves, De Angelis, Luther

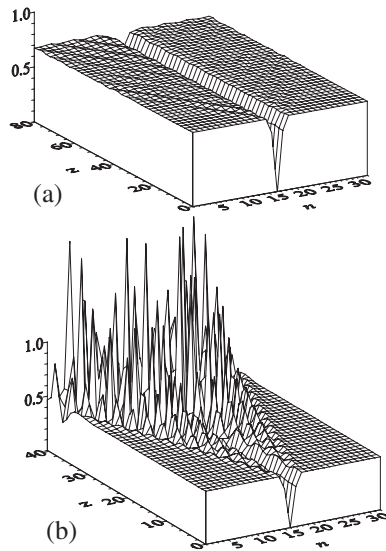


Fig. 10. Propagation of a dark, kink-like in-phase DS (the normalized FW intensity is shown). Parameters: $c_a = c_b = 0.1$, $\beta = -2$; (a) $b = -0.76 \rightarrow G_{\max} = 0$; (b) $b = -0.72 \rightarrow G_{\max} = 0.24$.

and Rubenchik [1994], Aceves, De Angelis, Luther, Rubenchik and Turitsyn [1995], Aceves, Luther, De Angelis, Rubenchik and Turitsyn [1995], Buryak and Akhmediev [1995], Laedke, Spatschek, Turitsyn and Mezentsev [1996] and Darmanyan, Relke and Lederer [1997]). The case of arrays with periodically modulated linear coupling was studied by Relke [1998].

The normalized slowly varying envelope b_n of the optical field in the n th channel of the waveguide array allowing for temporal dispersion is described by the dimensionless discrete–continuous nonlinear Schrödinger equation

$$i \frac{db_n}{dz} + s \frac{d^2 b_n}{dt^2} + c(b_{n-1} + b_{n+1}) + \lambda |b_n|^2 b_n = 0, \quad (5.25)$$

where t is the normalized time in the moving frame, and $s = 1$ or $s = -1$ stands for anomalous or normal group velocity dispersion, respectively. In this subsection we study the stability of a moving plane-wave solution to eq. (5.25) that may be written as

$$b_n(z, t) = b \exp[i(kz + qn - \omega t)], \quad (5.26)$$

where

$$k = \lambda |b|^2 + 2c \cos q - s\omega^2.$$

Here q is an arbitrary transverse wavevector and ω is the deviation from the carrier frequency.

We again perform the familiar linear stability analysis by modulating the unperturbed amplitude $b \rightarrow b + \psi_n(z, t)$ in eq. (5.26), where

$$\psi_n(t, z) = u \exp[i(Kz + Qn - \Omega t)] + v \exp[-i(K^*z + Qn - \Omega t)]. \quad (5.27)$$

Inserting eq. (5.26) into (5.25) we arrive at the dispersion relation for the perturbations:

$$(K + 2s\omega\Omega + 2c \sin Q \sin q)^2 = F(F - 2\lambda b^2), \quad (5.28)$$

where

$$F(\Omega, q, Q) = s\Omega^2 + 4c \cos q \sin^2(\frac{1}{2}Q). \quad (5.29)$$

Equation (5.28) straightforwardly gives the following expression for the MI gain:

$$\text{Im}[K] \equiv G = \sqrt{F(2\lambda b^2 - F)} > 0, \quad (5.30)$$

which varies with the wavenumber q of the stationary solution as well as with both the frequency Ω and wavenumber Q of the perturbation. In contrast, the real part of K additionally depends on the frequency ω of the carrier wave.

Two familiar limiting cases can be read off from eqs. (5.29) and (5.30) as MI of (i) the nonlinear Schrödinger equation (see, e.g., Abdullaev, Darmanyan and Khabibullaev [1993], Agrawal [1995]) for $c \cos q = 0$ (diffractionless case) and (ii) the discrete nonlinear Schrödinger equation for $s = 0$ (dispersionless case), see eq. (5.10).

It is obvious that the existence criterion, the domain and the gain of MI are essentially determined by $\text{sgn}(\lambda)$ and by $F(\Omega, q, Q)$ which, in turn, critically depends on the signs of both s and $\cos q$, see eq. (5.29). For example, in the case of defocusing, $\lambda = -1$, the MI occurs only for $-2b^2 < F < 0$, which is possible at (i) $s = 1$ (anomalous dispersion) and $\cos q < 0$ (negative “diffraction”) for the boundaries of the MI domain given by $\Omega_c^2 - 2b^2 < \Omega^2 < \Omega_c^2$, or at (ii) $s = -1$ (normal dispersion) and $\cos q \geq 0$ (positive/zero “diffraction”), in which case the MI domain is located in the frequency region $\Omega_c^2 + 2b^2 > \Omega^2 > \Omega_c^2$, or, lastly, at (iii) $s = -1$ (normal dispersion) and $\cos q \leq 0$ (negative/zero “diffraction”) for $2b^2 - \Omega_c^2 > \Omega^2$, where $\Omega_c^2 = 4c |\cos q| \sin^2(\frac{1}{2}Q)$. Detailed analyses of other cases as well as an analysis of the stability of a soliton array propagating in a waveguide array have been published by Darmanyan, Relke and Lederer [1997].

§ 6. Conclusions

In this review we have considered many aspects of the MI in inhomogeneous nonlinear media. The MI of electromagnetic waves in nonlinear optical fibers with periodic variations of amplification, dispersion or birefringence has been investigated. The MI in random media shows new properties such as the extension of fundamental MI domain to all frequencies of modulation and the existence of MI in the region of normal dispersion. Similar features can be observed in the MI in discrete nonlinear media.

It is desirable to perform experiments on the observation of MI in random nonlinear media. At present it seems that the best possibilities for realizing these experiments are in optical fibers with random parameters and in arrays of nonlinear polymer waveguides.

Some related problems have not been touched on in the review. First this concerns the MI of incoherent beams in nonlinear media. The investigation of this problem is important for understanding the conditions of existence of incoherent solitons, a phenomenon demonstrated in recent experiments (Mitchell and Segev [1997]). A second problem is the MI in fiber-ring soliton lasers with periodic dispersion. Recently, modulational instability with sideband generation in a passively mode-locked fiber-ring soliton laser has been observed by Tang, Man, Tam and Demokan [2000] and Tang, Fleming, Man, Tam and Demokan [2001]). The periodic modulation of dispersion was caused by the pulse circulating in the laser cavity. A promising perspective is the study of MI in periodically modulated quadratic media and in media with more complicated nonlinearities. Some preliminary results have been obtained by Corney and Bang [2001]. Another important direction is the MI in periodic media with higher dimensions. This is important for investigations of localized waves in nonlinear photonic crystals. The MI in 2D and 3D Bose–Einstein condensates in an optical lattice and the generation of localized states seems to be another significant problem for future studies. It should be of great interest to extend the approaches outlined in this review to the problem of MI in nonconservative modulated continuous media and discrete nonlinear optical systems with linear and nonlinear amplification or damping. The analysis of the regions of MI can be useful for the search of autosolitons both in continuous and in discrete media. Experimental observations of MI in a system possessing autosolitons, namely in a transmission system with periodic semiconductor amplifiers and in-line filters, have been reported by Goles, Darmanyany, Onishchukov, Shipulin, Bakonyi, Lokhnigin and Lederer [2000]. It is also interesting to investigate the long-time behavior of MI in modulated media. For this purpose it is necessary to go beyond

the linear stability analysis. One of the ways to do this analytically is to utilize the three-mode approximation. It has been shown that this approximation provides a good description of the complicated dynamics of MI under periodic perturbations of the medium. The theory of perturbations involving the dynamics of nonlinear periodic waves in periodic media needs to be developed. Recently, the existence of a new family of stationary nonlinear periodic solutions in NLSE with periodic potential has been reported by Bronski, Carr, Deconinck and Kutz [2001].

Acknowledgements

F.A. and S.D. appreciate valuable collaborations with F. Lederer, S. Bishoff, A. Kobayakov and M.P. Soerensen, our coauthors of original papers. S.D. and F.A. are grateful to US CRDF (Award ZM2-2095) for the partial financial support.

References

- Abdullaev, F.Kh., 1994, *Pisma Zh. Tech. Fiz.* **20**, 25.
- Abdullaev, F.Kh., 1999, in: *Optical Solitons*, eds V.E. Zakharov and S. Wabnitz, Les Houches (Springer/EDP Sciences, Heidelberg/Paris) pp. 51–61.
- Abdullaev, F.Kh., B.B. Baizakov, S.A. Darmanyan, V.V. Konotop and M. Salerno, 2001, *Phys. Rev. A* **64**, 043606.
- Abdullaev, F.Kh., J.G. Caputo and N. Flytzanis, 1994, *Phys. Rev. E* **50**, 1552.
- Abdullaev, F.Kh., S.A. Darmanyan, S. Bischoff and M.P. Sørensen, 1997, *J. Opt. Soc. Am. B* **14**, 27.
- Abdullaev, F.Kh., S.A. Darmanyan and P.K. Khabibullaev, 1993, *Optical Solitons* (Springer, Berlin).
- Abdullaev, F.Kh., S.A. Darmanyan, A. Kobayakov and F. Lederer, 1996, *Phys. Lett.* **220**, 213.
- Abdullaev, F.Kh., and J. Garnier, 1999, *Phys. Rev.* **E60**, 1042.
- Aceves, A.B., 2000, *Chaos* **10**, 584.
- Aceves, A.B., C. De Angelis, G.G. Luther and A.M. Rubenchik, 1994, *Opt. Lett.* **19**, 1186.
- Aceves, A.B., C. De Angelis, G.G. Luther, A.M. Rubenchik and S.K. Turitsyn, 1995, *Physica D* **87**, 262.
- Aceves, A.B., C. De Angelis, T. Peschel, R. Muschall, F. Lederer, S. Trillo and S. Wabnitz, 1996, *Phys. Rev. E* **53**, 1172.
- Aceves, A.B., G.G. Luther, C. De Angelis, A.M. Rubenchik and S.K. Turitsyn, 1995, *Phys. Rev. Lett.* **75**, 73.
- Agrawal, G.P., 1987, *Phys. Rev. Lett.* **59**, 880.
- Agrawal, G.P., 1995, *Nonlinear Fiber Optics*, 2nd Ed. (Academic Press, New York).
- Akhmediev, N.N., V.M. Eleonsky and N.E. Kulagin, 1990, *Selecta Math. Sov.* **9**, 215.
- Akhmediev, N.N., and V.I. Korneev, 1986, *Theor. Mat. Fiz.* **69**, 189 [*Theor. Math. Phys. (USSR)* **72**, 1089.]
- Anderson, P.W., 1958, *Phys. Rev. A* **109**, 1492.
- Bang, O., and P.D. Miller, 1996, *Opt. Lett.* **21**, 1105.
- Baxendale, P.H., and R.Z. Khaminskii, 1998, *Adv. Appl. Prob.* **30**, 968.

- Benjamin, T.B., and J.E. Feir, 1967, *J. Fluid. Mech.* **27**, 417.
- Berkhoer, A.I., and V.E. Zakharov, 1970, *Zh. Eksp. Teor. Fiz.* **58**, 903 [*Sov. Phys. JETP* **31**, 486].
- Bespalov, V.I., and V.I. Talanov, 1966, *Pisma JETP* **3**, 471 [*JETP Lett.* **3**, 307].
- Bronski, J.C., L.D. Carr, B. Deconinck and J.N. Kutz, 2001, *Phys. Rev. Lett.* **86**, 1402.
- Bronski, J.C., and J.N. Kutz, 1996, *Opt. Lett.* **21**, 937.
- Burlakov, V.M., 1998, *Phys. Rev. Lett.* **80**, 3988.
- Burlakov, V.M., S.A. Darmanyan and V.N. Pyrkov, 1995, *Sov. Phys. JETP* **81**, 501.
- Burlakov, V.M., S.A. Darmanyan and V.N. Pyrkov, 1996, *Phys. Rev. B* **54**, 3257.
- Buryak, A., and N.N. Akhmediev, 1995, *IEEE J. Quantum Electron.* **31**, 682.
- Cai, D.L., A.R. Bishop and N. Grønbech-Jensen, 1994, *Phys. Rev. Lett.* **72**, 591.
- Caputo, J.G., A.C. Newell and M. Shelley, 1990, in: *Integrable Systems and Applications*, eds M. Balabane, P. Lochak, D. McLaughlin and C. Sulem (Springer, Berlin).
- Corney, J.F., and O. Bang, 2001, *Phys. Rev. Lett.* **87**, 133901.
- Cristodoulides, D.N., and R.I. Joseph, 1988, *Opt. Lett.* **13**, 794.
- Darmanyan, S.A., A. Kobayakov and F. Lederer, 1998a, *Phys. Rev. E* **57**, 2344.
- Darmanyan, S.A., A. Kobayakov and F. Lederer, 1998b, *Sov. Phys. JETP* **86**, 682.
- Darmanyan, S.A., A. Kobayakov, E. Schmidt and F. Lederer, 1998, *Phys. Rev. E* **57**, 3520.
- Darmanyan, S.A., I. Relke and F. Lederer, 1997, *Phys. Rev. E* **55**, 7662.
- Daumont, I., T. Dauxois and M. Peyrard, 1997, *Nonlinearity* **10**, 617.
- De Sterke, C.M., 1998, *J. Opt. Soc. Am. B* **15**, 2660.
- De Sterke, C.M., and J.E. Sipe, 1990, *Phys. Rev. A* **42**, 550.
- Denardo, B., B. Galvin, A. Greenfield, A. Larraza, S. Putterman and W. Wright, 1992, *Phys. Rev. Lett.* **68**, 1730.
- Dolgov, A.S., 1986, *Phys. Solid State* **28**, 902.
- Doucot, B., and R. Rammal, 1987, *J. Phys.* **48**, 527.
- Eisenberg, H.S., Y. Silberberg, R. Morandotti, A.R. Boyd and J.S. Aitchison, 1998, *Phys. Rev. Lett.* **81**, 3383.
- Evangelides, S.G., L.F. Mollenauer, J.P. Gordon and N.S. Bergano, 1992, *J. Lightwave Technol.* **10**, 28.
- Fejer, M.M., G.A. Magel, D.H. Jundt and R.L. Byer, 1992, *IEEE J. Quantum Electron.* **26**, 1265.
- Flach, S., and C.R. Willis, 1998, *Phys. Rep.* **295**, 181.
- Gabitov, I., and S.K. Turitsyn, 1997, *Opt. Lett.* **21**, 327.
- Garnier, J., and F.Kh. Abdullaev, 2000, *Physica D* **145**, 65.
- Garnier, J., F.Kh. Abdullaev, E. Seve and S. Wabnitz, 2001, *Phys. Rev. E* **63**, 066616.
- Georges, T., 1998, *J. Opt. Soc. Am. B* **15**, 1553.
- Goles, M., S.A. Darmanyan, G. Onishchukov, A. Shipulin, Z. Bakonyi, V. Likhonin and F. Lederer, 2000, *Opt. Lett.* **25**, 293.
- Gordon, J.P., 1992, *J. Opt. Soc. Am. B* **9**, 91.
- Hasegawa, A., 1984, *Opt. Lett.* **9**, 288.
- Hasegawa, A., and Y. Kodama, 1995, *Solitons in Optical Communications* (Oxford University Press, Oxford).
- He, H., P.D. Drummond and B.A. Malomed, 1996, *Opt. Commun.* **123**, 394.
- Hennig, D., and G.P. Tsironis, 1999, *Phys. Rep.* **307**, 333.
- Infeld, E., 1981, *Phys. Rev. Lett.* **47**, 717.
- Infeld, E., and G. Rowlands, 1990, *Nonlinear Waves, Solitons and Chaos* (Cambridge University Press, Cambridge).
- Its, A.R., A.V. Rybin and M.A. Sall, 1988, *Theor. Math. Fiz.* **74**, 29. In Russian.
- Kaminow, I.P., 1981, *IEEE J. Quantum Electron.* **QE-17**, 15.
- Karlsson, M., 1998, *J. Opt. Soc. Am. B* **15**, 2269.

- Kelley, S.M., 1992, *Electron. Lett.* **28**, 806.
- Kikuchi, K., C. Lorattanasane, F. Futami and S. Kaneko, 1995, *IEEE Photonics Technol. Lett.* **7**, 1378.
- Kivshar, Yu.S., S.A. Gredeksul, A. Sánchez and L. Vázquez, 1990, *Phys. Rev. Lett.* **64**, 1693.
- Kivshar, Yu.S., M. Haelterman and A.P. Sheppard, 1994, *Phys. Rev. E* **50**, 3161.
- Kivshar, Yu.S., and M. Peyrard, 1992, *Phys. Rev. A* **46**, 3198.
- Klyatskin, V.I., 1980, *Stochastic Differential Equations and Waves in Random Media* (Nauka, Moscow).
- Knapp, R., 1995, *Phys. D* **85**, 496.
- Kobyakov, A., S.A. Darmanyan, F. Lederer and E. Schmidt, 1998, *Opt. Quantum Electron.* **30**, 795.
- Kobyakov, A., S.A. Darmanyan, T. Pertsch and F. Lederer, 1999, *J. Opt. Soc. Am B* **16**, 1737.
- Kodama, Y., A. Maruta and A. Hasegawa, 1994, *Quantum Semiclass. Opt.* **6**, 463.
- Konotop, V.V., and M. Salerno, 1997, *Phys. Rev. E* **56**, 3611.
- Konotop, V.V., and M. Salerno, 2002, *Phys. Rev. A* **65**, 021602-1.
- Krolikowski, W., and Yu.S. Kivshar, 1996, *J. Opt. Soc. Am. B* **13**, 876.
- Kurtzke, C., 1993, *IEEE Photon. Technol.* **5**, 1250.
- Kuwaki, N., and M. Ohashi, 1990, *J. Lightwave Technol.* **8**, 1476.
- Laedke, E.W., K.H. Spatschek, S.K. Turitsyn and V.K. Mezentsev, 1996, *Phys. Rev. E* **52**, 5549.
- Landau, L.D., and E.M. Lifshitz, 1973, *Mechanics* (Pergamon Press, Oxford).
- Lederer, F., S.A. Darmanyan and A. Kobyakov, 2001, in: *Spatial Solitons*, eds W. Torruellas and S. Trillo (Springer, Heidelberg) pp. 169–192.
- Leon, J., and M. Manna, 1999, *Phys. Rev. Lett.* **83**, 2324.
- Litchinister, N., C.J. McKinstrie, C.M. De Sterke and G.P. Agrawal, 2001, *J. Opt. Soc. Am. B* **18**, 45.
- Marquie, P., J.M. Bilbaut and M. Remoissenet, 1995, *Phys. Rev. E* **51**, 6127.
- Matera, F., F.A. Mecozzi, M. Romagnoli and M. Settembre, 1993, *Opt. Lett.* **18**, 1499.
- Middleton, D., 1960, *Introduction to Statistical Communication Theory* (McGraw-Hill, New York).
- Millar, P., J.S. Aitchison, J.U. Kang, G.I. Stegeman, A. Villeneuve, G.T. Kennedy and W. Sibbett, 1997, *J. Opt. Soc. Am. B* **14**, 3224.
- Miller, P.D., and O. Bang, 1998, *Phys. Rev. E* **57**, 6038.
- Millot, G., E. Seve, S. Wabnitz and M. Haelterman, 1995, *J. Opt. Soc. Am.* **B15**, 1266.
- Mitchell, M., and M. Segev, 1997, *Nature (London)* **387**, 880.
- Mollenauer, L.F., P.V. Mamyshev and M.J. Neubelt, 1996, *Opt. Lett.* **21**, 1924.
- Mollenauer, L.F., K. Smith, J.P. Gordon and C.R. Menyuk, 1989, *Opt. Lett.* **14**, 1219.
- Morandotti, R., U. Peschel, J.S. Aitchison, H.S. Eisenberg and Y. Silberberg, 1999, *Phys. Rev. Lett.* **83**, 2726.
- Murdoch, S.G., R. Leonhardt, J.D. Harvey and T.A.B. Kennedy, 1997, *J. Opt. Soc. Am. B* **14**, 1816.
- Nakajima, K., M. Ohashi and M. Tateda, 1997, *J. Lightwave Technol.* **15**, 1095.
- Ostrovski, L.A., 1966, *Zh. Eksp. Teor. Fiz.* **51**, 1189 [1967, *Sov. Phys. JETP* **24**, 797].
- Page, J.B., 1990, *Phys. Rev. B* **41**, 7835.
- Peschel, T., R. Muschall and F. Lederer, 1997, *Opt. Commun.* **136**, 16.
- Peschel, T., U. Peschel and F. Lederer, 1998, *Phys. Rev. E* **57**, 1127.
- Petrov, D.V., 1996, *Opt. Commun.* **131**, 102.
- Pötting, S., P. Meystre and E.M. Wright, 2000, *Atomic solitons in optical lattices*, eprint cond-mat/0009289.
- Rashleigh, S.C., 1983, *J. Lightwave Technol.* **1**, 312.
- Relke, I., 1998, *Phys. Rev. E* **57**, 6105.
- Revuz, D., and M. Yor, 1991, *Continuous Martingales and Brownian Motion* (Springer, Berlin).
- Schiek, R., Y. Baek and G.I. Stegeman, 1996, *Phys. Rev. E* **53**, 1138.

- Scott, A.C., 1992, Phys. Rep. **217**, 1.
- Shiraki, K., T. Omae and T. Horiguchi, 1998, in: Optical Fiber Communication Conference, Vol. 2 of OSA Technical Digest Series (Optical Society of America, Washington, DC) p. 356.
- Sievers, A.J., and S. Takeno, 1988, Phys. Rev. Lett. **61**, 970.
- Simon, A., and R. Ulrich, 1977, Appl. Phys. Lett. **31**, 517.
- Smith, M.J., and N.J. Doran, 1996, Opt. Lett. **21**, 570.
- Smith, N.J., F.M. Knox, N.J. Doran, K.J. Blow and I. Bennion, 1996, Electron. Lett. **32**, 54.
- Tai, K., A. Hasegawa and A. Tomita, 1986, Phys. Rev. Lett. **56**, 135.
- Tang, D.Y., S. Fleming, W.S. Man, H.Y. Tam and M.S. Demokan, 2001, J. Opt. Soc. Am. B **18**, 1443.
- Tang, D.Y., W.S. Man, H.Y. Tam and M.S. Demokan, 2000, Phys. Rev. A **61**, 023804.
- Torruellas, W.E., Z. Wang, D.J. Hagan, E.W. Van Stryland, G.I. Stegeman, L. Torner and C.R. Menyuk, 1995, Phys. Rev. Lett. **74**, 5036.
- Tracy, E.R., and H.H. Chen, 1984, Phys. Rev. A **37**, 815.
- Trillo, S., and P. Ferro, 1995, Opt. Lett. **20**, 438.
- Trillo, S., and S. Wabnitz, 1991, Opt. Lett. **16**, 986.
- Tsoy, E.N., C.M. De Sterke and F.Kh. Abdullaev, 2001, J. Opt. Soc. Am. B **18**, 1144.
- Van Simaey, G., Ph. Emplit and M. Haelterman, 2001, Phys. Rev. Lett. **87**, 033902.
- Vanossi, A., K.O. Rasmussen, A.R. Bishop, B.A. Malomed and V. Bortolani, 2000, Phys. Rev. E **62**, 7353.
- Vedenov, A.A., and L.I. Rudakov, 1964, Dokl. Akad. Nauk SSSR **159**, 767 [1965, Sov. Phys. Dokl. **9**, 1073].
- Wabnitz, S., 1988, Phys. Rev. A **38**, 2018.
- Wabnitz, S., Y. Kodama and A.B. Aceves, 1995, Opt. Fibre Technol. **1**, 187.
- Wai, P.K.A., and C.R. Menyuk, 1996, J. Lightwave Technol. **14**, 148.
- Wai, P.K.A., C.R. Menyuk and H.H. Chen, 1991, Opt. Lett. **16**, 1231.
- Winful, H.G., and G.D. Cooperman, 1982, Appl. Phys. Lett. **40**, 298.